(12) INTERNATIONAL APPLICATION PUBLISHED UNDER THE PATENT COOPERATION TREATY (PCT)

(19) World Intellectual Property Organization
International Bureau

(43) International Publication Date
08 November 2018 (08.11.2018)

WIPO | PCT

(10) International Publication Number
WO 2018/204388 A1

(51) International Patent Classification:
F24J 2/08 (2006.01) *H02S 20/32* (2014.01)
H01L 31/054 (2014.01) *H02S 40/22* (2014.01)

(21) International Application Number:
PCT/US2018/030491

(22) International Filing Date:
01 May 2018 (01.05.2018)

(25) Filing Language: English

(26) Publication Language: English

(30) Priority Data:
62/500,306 02 May 2017 (02.05.2017) US

(71) Applicant: **THE ARIZONA BOARD OF REGENTS ON BEHALF OF THE UNIVERSITY OF ARIZONA** [US/US]; The University of Arizona, Tech Launch Arizona, 220 West Sixth Street, Tucson, Arizona 85701 (US).

(72) Inventors: **ANGEL, Roger P.**; 933 North Cherry Avenue, Room 478, Tucson, Arizona 85721 (US). **HYATT, Justin J.**; The University of Arizona, Tech Launch Arizona, 220 West Sixth Street, 4th Floor, Tucson, Arizona 85701 (US). **RESHIDKO, Dmitry**; The University of Arizona, Tech Launch Arizona, 220 West Sixth Street, 4th Floor, Tucson, Arizona 85701 (US). **WHEELWRIGHT, Brian M.**; The University of Arizona, Tech Launch Arizona, 220 West Sixth Street, 4th Floor, Tucson, Arizona 85701 (US). **DIDATO, Nicholas J.**; The University of Arizona, Tech Launch Arizona, 220 West Sixth Street, 4th Floor, Tucson, Arizona 85701 (US).

(74) Agent: **THOREEN, Alexander C.**; Snell & Wilmer L.L.P., One Arizona Center, 400 East Van Buren Street, Phoenix, Arizona 85004-2202 (US).

(81) Designated States *(unless otherwise indicated, for every kind of national protection available)*: AE, AG, AL, AM, AO, AT, AU, AZ, BA, BB, BG, BH, BN, BR, BW, BY, BZ,

(54) Title: SOLAR PV GENERATOR WITH DISH REFLECTOR AND FLY'S EYE RECEIVER

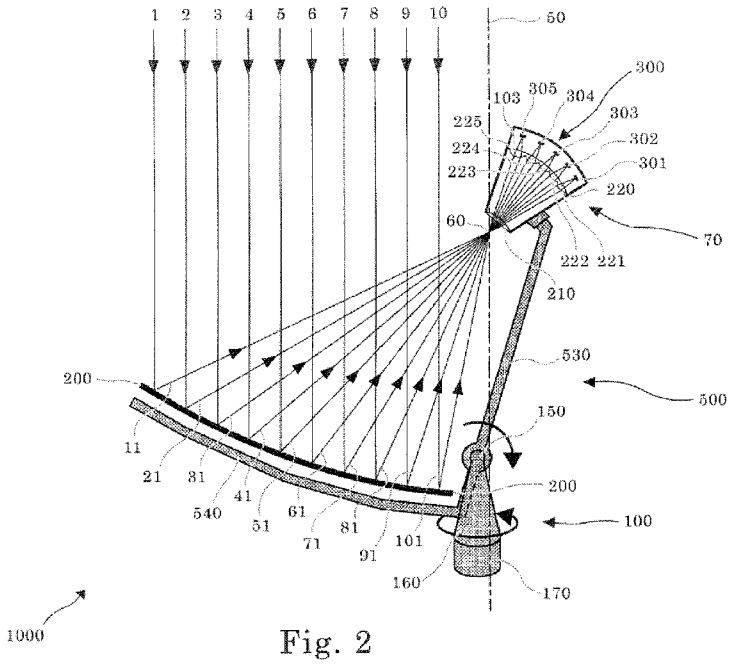


Fig. 2

(57) Abstract: An apparatus for generating electricity from solar energy has a large dish reflector with a fly's eye receiver positioned near the focus of the dish reflector, held by a dual axis tracking structure. The fly's eye receiver includes a field lens that concentrates sunlight into an image of the dish reflector, a two-dimensional fly's eye array of contiguous convex lenses extending across the dish image, and a photovoltaic cell behind each convex lens of the fly's eye array. Two imaging stages are provided. First, the dish reflector and the field lens concentrate the sunlight in the form of an image of the dish that is stabilized against pointing errors of the tracking mechanism. Second, the contiguous array of convex lenses divides the sunlight energy of the dish image into portions, one per convex lens, each portion being further concentrated by the respective convex lens onto a corresponding photovoltaic cell.

WO 2018/204388 A1

[Continued on next page]

CA, CH, CL, CN, CO, CR, CU, CZ, DE, DJ, DK, DM, DO, DZ, EC, EE, EG, ES, FI, GB, GD, GE, GH, GM, GT, HN, HR, HU, ID, IL, IN, IR, IS, JO, JP, KE, KG, KH, KN, KP, KR, KW, KZ, LA, LC, LK, LR, LS, LU, LY, MA, MD, ME, MG, MK, MN, MW, MX, MY, MZ, NA, NG, NI, NO, NZ, OM, PA, PE, PG, PH, PL, PT, QA, RO, RS, RU, RW, SA, SC, SD, SE, SG, SK, SL, SM, ST, SV, SY, TH, TJ, TM, TN, TR, TT, TZ, UA, UG, US, UZ, VC, VN, ZA, ZM, ZW.

(84) Designated States *(unless otherwise indicated, for every kind of regional protection available)*: ARIPO (BW, GH, GM, KE, LR, LS, MW, MZ, NA, RW, SD, SL, ST, SZ, TZ, UG, ZM, ZW), Eurasian (AM, AZ, BY, KG, KZ, RU, TJ, TM), European (AL, AT, BE, BG, CH, CY, CZ, DE, DK, EE, ES, FI, FR, GB, GR, HR, HU, IE, IS, IT, LT, LU, LV, MC, MK, MT, NL, NO, PL, PT, RO, RS, SE, SI, SK, SM, TR), OAPI (BF, BJ, CF, CG, CI, CM, GA, GN, GQ, GW, KM, ML, MR, NE, SN, TD, TG).

Published:

— *with international search report (Art. 21(3))*

— *before the expiration of the time limit for amending the claims and to be republished in the event of receipt of amendments (Rule 48.2(h))*

SOLAR PV GENERATOR WITH DISH REFLECTOR AND FLY'S EYE RECEIVER

FIELD

[0001] The present invention relates to the generation of solar electrical power using a large dish reflector to power multijunction photovoltaic cells.

BACKGROUND

[0002] In the past, single junction photovoltaic ("PV") cells have been widely used to convert sunlight into electricity. The efficiency of conversion of the total amount of incident solar energy is at best a little more than 20% conversion in current commercial PV modules. This limitation on the efficiency of conversion arises because conventional PV modules use a single semiconductor type. While any given semiconductor may convert with high efficiency at a given characteristic wavelength, it is less efficient at other wavelengths across the solar spectrum, and typically can convert only a small amount of the available solar energy into electricity.

[0003] A PV system with higher efficiency across the spectrum is preferred over a conventional module, provided the overall cost is not increased so much as to offset the efficiency gain. Sunlight may be converted into electricity with higher overall efficiency than is possible with any one semiconductor, by dividing the solar spectrum and using the different parts to power a PV cell comprising two or more semiconductors, each cell being illuminated preferentially by those parts of the spectrum which it converts with highest efficiency. The different semiconductors may be stacked on top of each other, forming a multijunction cell. In a multijunction cell, different spectral bands separate out by absorption as sunlight travels down through the stack. Multijunction cells have been commercially developed and are widely used to power spacecraft. However, this multijunction approach is limited to expensive semiconductors and manufacturing techniques. To reduce the overall cost, for terrestrial energy generation a small multijunction cell may be used in conjunction with optics which collect a larger area of direct sunlight and strongly focus it onto the smaller cell area.

[0004] Operated under sunlight at high concentration, such cells may realize twice the conversion efficiency of conventional cells and, since a much smaller cell area is needed to convert sunlight that has been highly concentrated, cell cost may be several times less than conventional PV cells, per unit of power output.

[0005] In the past, there have been solar generators that aimed at exploiting the very high efficiency of multi-junction solar cells where the solar generators employed many small focusing optical systems, each one focusing incoming sunlight onto a single small cell. Typically, many optical systems and cells were assembled into a module. The cells were typically cooled by natural convection, requiring a substantial mass of thermal conductor, such as aluminum. However, such assemblies, which include individual focusing optics, concentrators, cells, heatsinks and supporting structure, tended to be large, heavy and complex, driving up cost of manufacture and transportation. Also the most commonly used focusing optic, a Fresnel lens, loses some light by scattering and has chromatic aberration, which may upset the spectral balance of focused sunlight, and both effects contribute toward a reduced conversion efficiency. Overall costs of electrical energy generated by installations having such large, heavy and complex concentrating photovoltaic ("CPV") modules have not proved competitive with those using conventional PV modules.

[0006] In the past, some designs of CPV generators have been disclosed that avoid the complexity and cost of large CPV modules by collecting sunlight with a single large focusing dish reflector and focusing it onto a small package containing many multi-junction photovoltaic cells in a densely packed array. One example is U.S. Patent Application No. 2011/0168234, to Lasich. Such systems may however suffer from uneven distribution of concentrated sunlight among the cells, especially if the solar tracking is not accurate. Uneven distribution of sunlight leads to loss of efficiency. Efficiency is also reduced when cells are packaged close together to form a dense array, because light is lost in any gaps between the cells and at light-insensitive electrical busbars at the cell perimeter.

[0007] A dish-based concentrating photovoltaic solar generator that mitigates many of these difficulties has been disclosed by Angel in U.S. Patent No. 8350145B2, and by Angel *et al.*, in U.S. Patent Application No. US 2015/0303867 A1. In these inventions, a spherical or other short focus lens, preferably of fused silica, is introduced near the focus of a paraboloidal dish to image the dish at high concentration onto an array of slightly separated cells. Secondary roof reflectors between the cells direct the light away from the gaps between the cells and onto their photovoltaically active areas. However, some practical difficulties that increase cost may remain. One is that the secondary reflectors may absorb a few percent of the highly concentrated sunlight to which they are exposed, reducing efficiency, and they may need active cooling, increasing complexity. Efficiency and tolerance to mispointing may also be reduced by the increased angles of incidence on the

cells of the reflected light. The short focus fused silica lens placed near the dish focus may also present some difficulties: it may have steeply curved surfaces and be thick, increasing weight and cost. Also its steep curvature may cause strong spherical aberration. As a result, if the dish is inadvertently mispointed, focused sunlight entering toward the edge of the lens may be refracted away from the cells and present a problem for thermal management. A further difficulty has been in minimizing the reflection losses of a silica lens over the very broad spectral band of multijunction cells. Additional difficulties may arise from there being little room to space the cells apart, especially if they are small, as preferred for high efficiency. As a result, wiring between the cells may be constricted. Also, cooling of closely spaced cells may be complicated by the high average density of heat to be removed, requiring pumped liquid coolant that may add further to complexity and cost.

[0008] In the past, the cost of the dual axis trackers used to orient CPV generators to the sun has been relatively high, and has contributed to their not being commercially competitive with electrical generation by PV panels on single axis trackers. The dual axis trackers used have been almost exclusively used on a post surmounted by a slewing bearing to provide azimuthal rotation. Such mountings are also used extensively for heliostats for thermal generation.

[0009] However, dual axis trackers of this type have employed heavy steel construction in an attempt to prevent damage by strong forces and moments from rare strong winds. In an effort to realize a more efficient tracker that spreads the load more broadly to reduce stresses and moments, and hence mass and cost, in the past, dual axis trackers have been proposed in which azimuth motion is made by wheels turning on a circular track, with the potential for a more efficient structure with less mass and cost.

[0010] Vindum (U.S. Patent No. 4,256,088) describes a wheeled dual axis tracker with a solar reflector structure supported in part from a circular rail, and in part from a central ground foundation by a telescoping linear actuator. The rail supports the elevation axis on a wheeled rotating structure which takes most of the weight when the reflector structure points to the horizon, while a hydraulic actuator drives the structure in elevation, taking most of its weight when the reflector structure points to the zenith. A problem with this design is that the requirement of long extension required of the linear actuator leads to the use of hydraulics in a multi-section unit, driving up capital and maintenance costs.

[0011] Another design for a dual axis solar tracker that turns on wheels on a rail is described by Moore (U.S. Patent No. 4,649,899). In this case, the elevation axis is supported

on a square structure with 4 wheels, and the elevation drive is via a screw actuator on the square structure. Yet another design for a rail-mounted tracker is by Angel and Davison (U.S. Patent No. 8,430,090).

[0012] A common deficiency of the above rail track designs is the mass and cost of the steel rail used to constrain lateral translation of the tracker.

[0013] A design that avoids the need for a rail, and uses a flat circular track on the ground, has been described by Cabanillas (U.S. Patent No. 8,237,098). In this design, a wheeled dual axis tracker is supported in part by the circular track and in part by a central support that takes some of the vertical load and also constrains lateral motion, avoiding the need for a rail. The design has four wheels, one projecting forward (a nose wheel). To avoid distortion of the four-wheeled rotating structure by irregularities in the circular track, the structure is articulated, with articulated lattice girders reaching out to the four wheels. The girders are hinged at the center post to accommodate vertical displacements of the wheels. But these features have driven up complexity and cost, making this design uncompetitive in practice.

[0014] In view of these challenges and difficulties, the long-felt need for better efficiency of solar conversion at lower cost, and to simplify and reduce the cost of dual axis tracker support, continues to leave room for improvement over the prior art.

SUMMARY

[0015] It is an object of the present invention to improve the efficiency and reduce the production cost of PV solar electricity generators, by concentrating sunlight in a two-stage process before its conversion into electricity by small, highly efficient multijunction PV cells. Such two-stage concentration allows the collection function to be performed by a large, inexpensive reflector mounted on a lightweight tracker, while division of the collected sunlight into equal portions for each of the cells, (for simple and efficient series electrical connection), is made not on its first entering the system, as is the case for nearly all past PV and CPV systems, but at smaller scale following the first stage of concentration. It is an object to package the small cells and apportioning optics into a receiver module that is smaller and less expensive to manufacture than a conventional PV panel or CPV module of the same power, and which may also be upgraded at low cost. The receiver is co-mounted with a large area concave dish reflector on a dual axis tracker. It is a further object that the optical system use imaging optics exclusively to concentrate the sunlight in the first stage of

concentration, so as to preserve optical etendue and thus minimize losses from tracker mispointing. It is also an object to manufacture the lenses in a way that minimizes surface reflection losses, so as to maximize optical throughput and system efficiency. It is further an object that optics provide for sufficient separation between the individual multijunction cells so as to facilitate electrical wiring, and also to reduce the heat flux averaged across the cell array, so that if thermal output is not required, forced air convection may be advantageously used to cool the cells rather than recirculated liquid.

[0016] It is a further object of the present invention to provide a dual axis tracker design that is structurally more efficient in its use of steel, and inexpensive to manufacture and install in the field.

[0017] In accordance with the present invention, a solar electric generator is disclosed in which sunlight is concentrated in two successive stages onto multi-junction PV cells. The first stage of concentration is accomplished by a large, concave reflector acting together with a field lens near its focus that forms the entrance to a small receiver. A stabilized pupil image of the reflector formed within the receiver by the field lens marks the first stage of concentration, which may be approximately 10 – 50 times that of natural sunlight. After this first stage of concentration, the area of concentrated light has a sharp and stable boundary, facilitating division onto PV cells.

[0018] In accordance with the present invention, the second stage of concentration is made by a “fly’s eye” lens array. For purposes of this invention, a “fly’s eye” lens array is a multiplicity of contiguous small convex lenses located at said pupil image. As in a compound insect eye, each lens of the fly’s eye lens array focuses light on a receptor behind. In our case, the receptors are small, separated multijunction PV cells. The lenses are individually sized in order to apportion the light from the pupil image in equal amounts to the multijunction cells. The additional second stage concentration, provided by each lens of the array focusing light down onto the cell behind, may be a factor of 10 – 50. The total concentration from both stages operating together is thus in the range of approximately 100 – 2500.

[0019] The field lens near the dish focus and the subsequent fly’s eye lens array and multijunction PV cells are packaged together to form a small receiver. The receiver and the large dish reflector are rigidly held in co-alignment, the assembly being oriented to the sun through the day by a dual axis tracker.

[0020] The large concave reflector in this generator is preferably an off-axis section of a paraboloidal dish, configured so that the fly's eye receiver does not obscure the sunlight coming into the reflector. The reflector may be assembled from one or more off-axis shaped mirror segments on a supporting structure. The focal ratio of the off-axis paraboloid, *i.e.*, the ratio of its focal length to its diameter (or width if not circular), may be chosen to be in the range f/0.5 to f/2. One or more reflectors, each with a receiver at its focus, may be carried on one dual-axis tracker.

[0021] In accordance with the present invention, the fly's eye receiver placed near the reflector focus has a field lens at its entrance. This lens forms a pupil image of the reflector on the fly's eye lens array. The optical power of the field lens is chosen according to the desired amount of first stage optical concentration at the fly's eye lens array. For example, if an average concentration of 25x is desired, the pupil image formed by the lens must be about 1/5 the size of the primary concave reflector. The field lens forms a pupil image of the reflector on a concave surface, whose position and light distribution is largely stabilized against tracker mispointing. The diameter of the field lens will depend on the focal ratio of the primary reflector and the desired angular acceptance for mispointing for the first stage of concentration. For example, if the primary focal ratio is f/1 and the mispointing tolerance is ± 1°, then the diameter of the field lens must be at a minimum 1/25 that of the reflector, depending on the positioning of the lens. The field lens may form a sealed entrance window to an enclosure that protects the following optics and cells against moisture and soiling.

[0022] Within the fly's eye receiver, the first-stage concentrated sunlight formed as a pupil image by said field lens is divided and further concentrated in a second stage by the fly's eye lens array. The array may have overall an approximately concave spherical shape, the center of said sphere being near the field lens. Such centration will ensure that the rays of first-stage concentrated sunlight entering any one of the lenses of the array will, when there is no pointing error, be aligned with the axis of that lens, and will be brought to a focus on that axis. The lenses of the fly's eye array are made contiguous, with minimal loss at gaps between the lenses, so that virtually all the first stage concentrated sunlight energy at the pupil is divided and transmitted by the fly's eye array for second stage concentration onto the cells.

[0023] Since the flux of concentrated light after the first stage varies uniformly across the array, being strongest at the furthest point from the parent paraboloid axis, the lenses are sized with different areas so that the sunlight power focused by any individual lens is the

same for all. The electrical current from all the cells will then be substantially the same, allowing for efficient series connection.

[0024] The PV cells at the focus of each lens of the fly's eye array may be of the multijunction type, to provide very high efficiency conversion of highly concentrated sunlight into electricity. The cells may be small, 6 mm or smaller, to minimize electrical Joule losses. As an example, 5 mm square cells might be illuminated by 25 mm square fly's eye lenses. The second stage concentration, the ratio of the lens to cell areas, would then be 25x.

[0025] Each cell may be operated directly at or near the focus of a fly's eye lens. Alternatively, a tertiary optical element such as a dome lens or optical funnel may be placed in optical contact with or directly above each cell, to more uniformly distribute the concentrated light across the cell, and also to increase mispointing tolerance. A dome lens may form an image on the lens element of the fly's eye array that precedes it.

[0026] Both the dome lenses and the fly's eye lenses will preferably have high transparency across the parts of the solar spectrum which are converted by the multijunction cells, so as to avoid spectral imbalances and loss of power. Also, their absorption at longer wavelengths of the solar spectrum should preferably be low enough to avoid significant heating of the lenses.

[0027] Minimizing surface reflection at the field lens is key to maintaining high optical transmission and overall conversion efficiency of this invention. It may be accomplished by an advanced coating process disclosed in this invention, in which double sol-gel layers provide very low reflection loss over the very wide spectral bandwidth of multi-junction PV cells.

[0028] Very low reflection at the surfaces of the fly's eye and dome lenses, in addition to the field lens, is important to maintaining high optical transmission and overall conversion efficiency of this invention. It may be preferably accomplished by making these lenses of borosilicate glass that has been phase separated and then leached in acid. This process is described below as part of this disclosure, but the described process may have advantageous applications that are independent of the solar energy generator described herein.

[0029] The cells and dome lenses may be mounted individually on ceramic circuit cards which combine high electrical resistance and thermal conductivity. The electrical outputs from the circuit cards may be connected in series.

[0030] To ensure that the cells operate at highest efficiency, they are preferably cooled. Heat generated in the cells by the concentrated sunlight may be conducted away through the

ceramic circuit cards and through a concave bowl of high conductivity material, such as aluminum or copper. The bowl may also form the supporting structure of the fly's eye receiver, holding the cell circuit cards and tertiary optical elements correctly centered under the lenses. The conductive bowl may be cooled from behind either by a heat transfer fluid, or by forced air convection acting on finned structures. Convective air cooling from behind is enabled by the relatively low heat density of the first stage of concentration of this invention. In this invention, the heating at the conductive supporting structure is set by the average concentration which may be only 25x, compared with 600x if the cells were densely packed. Thus, one advantage of the present invention is the relatively low heat density properties of this approach to concentration, which has cost advantages and favorable operational characteristics.

[0031] In accordance with the present invention, a dual axis tracker of elevation over azimuth design is provided that minimizes cost of manufacture and field installation. Its azimuth structure is a rigid triangular spaceframe supported at its three corners by wheels, one or more being driven. Four of the six degrees of freedom of rigid body motion of the azimuth structure are constrained by the position of the wheels on the track: vertical displacement (z), tip, tilt and azimuth rotation. A central ground bearing constrains the remaining two degrees of motion, namely lateral displacement (x and y). The central bearing also restrains upward motion in high wind, but takes no downward load. In this design, the azimuthal rotation axis may be as much as several degrees off vertical, and the track not especially flat, to reduce cost, nevertheless any orientation needed for heliostat or sun pointing may be achieved by choosing the correct angles of rotation around the track and about the elevation axis. To allow accurate tracking as a heliostat, the tracker may be provided with level sensors and encoders for elevation and rotation about the central bearing. For direct pointing to the sun, as needed for the fly's eye generator, a sun position sensor is provided. To reduce the cost of on-site assembly, the spaceframe structures will be largely prefabricated and shipped as major flat subassemblies with premanufactured nodes, to be connected with the lightweight struts in the field.

BRIEF DESCRIPTION OF THE DRAWINGS

[0032] Figure 1 is a perspective view of a preferred embodiment of the invention with adjacent large square reflectors and receivers.

[0033] Figure 2 is a schematic cross-sectional view of one of the square reflectors and the associated receiver of Figure 1, showing paths of on-axis rays in a preferred embodiment of the generator.

[0034] Figure 3 is a perspective view of a fly's eye lens array.

[0035] Figure 4 is a schematic cross-section of the generator shown in Figure 2, with the addition of off-axis rays.

[0036] Figure 5 shows a partial view of magnified detail of the receiver shown in Figure 4.

[0037] Figure 5a is a diagram showing rays brought to a focus by differently sized elements of the fly's eye array.

[0038] Figure 6 is a detailed plan view illustrating the focusing of on-axis rays and off-axis rays, as seen from the field lens.

[0039] Figure 7a shows rays before the addition of a dome lens placed on a cell.

[0040] Figure 7b shows rays after the addition of a dome lens placed on a cell.

[0041] Figure 7c shows a magnified plan view of the photovoltaic cell shown in Figure 7a, illustrating in more detail the central focus of sunlight for on-axis rays, and the displaced focus of sunlight for off-axis rays, in an example illustrating the effects of mispointing without a dome lens.

[0042] Figure 7d shows a magnified plan view of the photovoltaic cell shown in Figure 7b, illustrating in more detail the focus of sunlight for on-axis rays, and the focus of sunlight for off-axis rays, in an example illustrating the effects of mispointing with a dome lens.

[0043] Figure 7e shows rays after the addition of an optical funnel placed on a cell.

[0044] Figure 7f shows a magnified plan view of the photovoltaic cell shown in Figure 7e, illustrating in more detail the focus of sunlight for both on- and off-axis rays, in an example illustrating the effects of mispointing with a funnel lens.

[0045] Figure 8a shows schematically a side view of a cooled single cell with a dome lens, and illustrates how heat generated in a cell may be removed by conduction and forced convection.

[0046] Figure 8b shows schematically a side view of a cooled single cell with a dome lens, and illustrates an alternative method of cooling in which a thermal transfer liquid flows behind and in thermal contact with a support element.

[0047] Figure 9 illustrates light loss mechanisms in the receiver.

[0048] Figure 10a shows an apparatus for coating a fused silica lens.

[0049] Figure 10b shows the measured reflectivity of a coated fused silica surface.

[0050] Figure 11 shows the measured reflectivity of a treated borosilicate glass surface.

[0051] Figure 12 shows the spectral absorption of light by a plate 19 mm thick plate of commercial borosilicate glass.

[0052] Figure 13a shows a lens with a convex aspheric upper surface.

[0053] Figure 13b shows the single lens illustrated in Figure 13a, which has been cut to the correct shape to fit as an element of the fly's eye lens array.

[0054] Figure 13c shows a portion of the fly's eye lens array which is made by fitting together a plurality of cut lenses that were cut as shown in Figure 13b.

[0055] Figure 13d is a schematic diagram of the supporting structure for a fly's eye array.

[0056] Figure 13e shows slotted arcs for assembly into a slotted egg crate structure.

[0057] Figure 13f shows a detail of matching slots and tabs for lens positioning.

[0058] Figure 13g is a ray diagram showing how refracted rays are not blocked by the support structure.

[0059] Figure 14a is a schematic diagram illustrating a step in the manufacture of the fly's eye lens array by one-piece array molding, where the first part of the mold is quilted with the inverse shape of the desired fly's eye lens array or subarray.

[0060] Figure 14b is a schematic diagram illustrating a step in the manufacture of the fly's eye lens array by one-piece array molding, where the second part of the mold is concave with grooves cut radially to take the squeezed out glass.

[0061] Figure 14c is a cross-sectional view illustrating a step in the manufacture of the fly's eye lens array by one-piece array molding, where the just-formed and still relatively soft molded glass is supported by the concave second lower side of the mold.

[0062] Figure 15a shows a ray trace diagram for a specific first stage concentrator.

[0063] Figure 15b shows a ray trace diagram for the same specific first stage concentrator referenced in Figure 15a.

[0064] Figure 16 shows a footprint diagram for rays at the pupil image.

[0065] Figure 17a shows a plan view of a generator configured with two off-axis paraboloidal reflectors and their respective fly's eye receivers.

[0066] Figure 17b shows a side view of the generator illustrated in Figure 17a.

[0067] Figure 18 is a plan view of an alternative generator with two adjacent mirrors.

[0068] Figure 19 shows a ray trace diagram for first stage concentrator of the alternative generator referenced in Figure 18.

[0069] Figure 20 shows a raytrace diagram detailing the receiver referenced in Figure 18.

[0070] Figure 21 shows a footprint diagram for on-axis and off-axis rays at the pupil image location of the fly's aye array.

[0071] Figure 22 shows a dual axis tracker with a flat reflector in a preferred embodiment of this invention.

[0072] Figure 23 shows the dual axis tracker of Figure 22 at the same elevation but rotated about the track, to show the front of the reflector surface.

[0073] Figure 24 shows a detail of the connection between the central ground anchor and the rotating structure.

[0074] Figure 25 shows a dual axis tracker carrying two dish reflectors and additions to the elevation structure to support fly's eye receivers.

DETAILED DESCRIPTION

[0075] **Figure 1** is a perspective view of a preferred embodiment of the invention, a generator **1000** with two adjacent large square reflectors **201** and **202.** Sunlight rays striking the first reflector **201,** such as rays **1, 2, 3** and **4,** are focused into a first receiver **722**, where they are converted into electricity. Similarly rays striking the second reflector **202**, such as rays **5, 6,** 7 and **8,** are focused into a second receiver **72**. The first and second receivers **722** and **72** are fixed in position relative to the first and second reflectors **201** and **202**, respectively, by a first arm **531** and a second arm **532**, and are positioned to receive all reflected rays, but are positioned below any incoming rays. For example, the first receiver **722** is position so that it receives reflected ray **1b** without blocking incoming ray **1a**. Similarly, the first receiver **722** is position so that it receives reflected ray **2b** without blocking incoming ray **2a**.

[0076] The assembly of reflectors, receivers and connecting supports together comprise the elevation structure **500**, which is oriented to the sun by azimuth and elevation bearings (not visible in **Figure 1**) supported atop a fixed post or support **170**.

[0077] **Figure 2** is a schematic cross section showing light ray paths in a preferred embodiment of a solar generator **1000** according to the present invention. The receiver **70** illustrated in **Figure 2** may represent either the first receiver **722** or the second receiver **72**

shown in **Figure 1**, because both the first receiver **722** and the second receiver **72** are preferably the same. As shown in **Figure 2**, entering parallel rays of light **1, 2, 3, 4, 5, 6, 7, 8, 9**, and **10**, respectively, strike the reflector **200** and are directed and concentrated into the receiver **70**. With the generator correctly oriented to the sun, entering rays **1, 2, 3, 4, 5, 6, 7, 8, 9**, and **10**, respectively, strike the reflector **200**, and are reflected as reflected rays **11, 21, 31, 41, 51, 61, 71, 81, 91**, and **101**, respectively. Reflected rays **11, 21, 31, 41, 51, 61, 71, 81, 91**, and **101**, respectively, enter the receiver **70** through a lens **210** and pass through a fly's eye lens array **220**, to be converted into electricity by a plurality of photovoltaic cells **301, 302, 303, 304**, and **305**. For convenience, the photovoltaic cells **301, 302, 303, 304**, and **305** will sometimes be referred to merely as "cells," it being understood by persons skilled in the art in the context of this description that a "cell" refers to a photovoltaic cell, or in a preferred embodiment, more specifically a multijunction photovoltaic cell.

[0078] The rigid elevation structure **500** holds the fly's eye receiver **70** at a substantially fixed orientation to the reflector **200**. The rigid elevation structure **500** comprises a mirror support **540** connected to the receiver **70** by an arm **530**. The rigid elevation structure **500** may be rotated to orient the generator to the sun, as the sun moves during the day, by a dual-axis tracking mount **100** set upon a fixed support **170.** Rotation about a horizontal axis is by an elevation bearing **150**, which in turn is rotated about a vertical axis by an azimuth bearing and drive **160**.

[0079] In a preferred embodiment, the entering reflector **200** is an off-axis segment of a paraboloid with axis **50**, causing the rays **1, 2, 3, 4, 5, 6, 7, 8, 9**, and **10**, shown parallel to the axis **50,** to converge to the focus **60** of the paraboloid, as indicated in **Figure 2** by converging rays **11, 21, 31, 41, 51, 61, 71, 81, 91**, and **101.** The entering reflector **200** is located to the side of the paraboloid axis **50** so that, as shown, the incoming sunlight rays **1, 2, 3, 4, 5, 6, 7, 8, 9**, and **10**, are not blocked by the fly's eye receiver **70.**

[0080] The entering rays of sunlight **1, 2, 3, 4, 5, 6, 7, 8, 9**, and **10**, as shown in **Figure 1**, are shown equally spaced to represent equal amounts of sunlight power. These rays after striking the reflector **200** are reflected to a focus **60** as rays **11, 21, 31, 41, 51, 61, 71, 81, 91,** and **101**, respectively. These reflected rays **11, 21, 31, 41, 51, 61, 71, 81, 91,** and **101**, enter the receiver **70** through the field lens **210**.

[0081] The receiver lenses include the field lens **210** and the fly's eye lens array **220**. The receiver lenses (the field lens **210** and the fly's eye lens array **220)** in this invention are configured so as to divide all the entering focused sunlight power into a multiplicity of equal

portions, each portion directed to an individual multijunction cell **301, 302, 303, 304**, and **305**, respectively, for conversion into electricity.

[0082] In conventional PV modules with no concentration, equal division is accomplished by making large PV cells of equal size, and placing them close together to avoid wasting sunlight. In the receiver **70** of this invention, the division of entering sunlight into equal portions is accomplished by the fly's eye lens array **220**. In the example of the fly's eye lens array **220** illustrated in **Figure 2**, a plurality of individual lenses **221, 222, 223, 224,** and **225**, are shown. For the sake of clarity, only five individual lenses **221, 222, 223, 224,** and **225**, are shown in **Figure 2**, it being understood by those skilled in the art that a full fly's eye lens array **220** would include a square array of more individual lenses, as shown in **Figure 3**. Referring to **Figure 2**, the individual lenses **221, 222, 223, 224,** and **225** are differently sized so each one intercepts the same amount of sunlight power. Those lenses **221, 222, 223, 224,** and **225** furthest from the paraboloid parent axis, where the optical flux is highest, are the smallest. The individual lens elements **221, 222, 223, 224,** and **225** are closely abutted on all sides, with only the smallest gaps between them, to minimize loss of light. Because of the focusing action of the individual lenses **221, 222, 223, 224**, and **225**, in the fly's eye lens array **220**, the small multijunction cells **301, 302, 303, 304** and **305**, behind the individual lenses **221, 222, 223, 224**, and **225**, respectively, are conveniently spaced apart, simplifying electrical connections and thermal management.

[0083] **Figure 3** is a perspective view showing an example of a full fly's eye lens array **220** according to this invention, as might be matched to the pupil image of a square entering reflector **200**, which image is formed by the field lens **210**. In this preferred example, the individual lenses, such as individual lenses **221, 222, 223, 224** and **225**, are approximately square and form part of a quilted, first surface **250**, or upper surface **250**.

[0084] In a preferred embodiment of this invention, the overall shape **251** of the fly's eye lens array **220** generally conforms to part of the surface of a sphere whose center is near the center of the field lens **210**, and whose perimeter best coincides with the perimeter of the reflector image formed by the field lens **210**. The axes of each individual lens **221, 222, 223, 224**, and **225**, is oriented toward the center of the field lens **210**. When the generator is correctly oriented to the sun, such a configuration ensures that the rays of concentrated sunlight refracted by each and every one of the lenses **221, 222, 223, 224**, and **225**, of the fly's eye lens array **220**, will be brought to a focus centered on that respective lens axis and

on one of the PV cells **301, 302, 303, 304**, and **305**, respectively, in the cell array **300** behind the fly's eye lens array **220**.

[0085] **Figure 4** shows the same entering rays **1, 2, 3, 4, 5, 6, 7, 8, 9**, and **10**, of **Figure 2**, all parallel to the optical axis **50** and reflected to the on-axis focus **60**. But in addition, represented by dashed lines, **Figure 4** shows another set of rays **111, 12, 13, 14, 15, 16, 17, 18, 19**, and **110**, parallel to each other, but entering at a slight angle **δ** to the optical axis **50,** as would be the case in the event of mispointing. These rays **111, 12, 13, 14, 15, 16, 17, 18, 19**, and **110**, are reflected from the reflector **200** at the same regularly spaced points **2001, 2002, 2003, 2004, 2005, 2006, 2007, 2008, 2009**, and **2010**, as the on-axis rays **1, 2, 3, 4, 5, 6, 7, 8, 9**, and **10**, but are brought to a displaced focus **601**, which is no longer centered upon the field lens **210**, but instead is offset displaced to the right of the on-axis focus **60** at point **601** as shown in **Figure 4**.

[0086] **Figure 5** shows a detail of the same on-axis rays and off-axis rays of **Figure 4** as they pass through the receiver **70**. We see that, after refraction by the field lens **210**, off-axis rays originating at the same point on the primary reflector and passing through the displaced focus **601** end up at the same positions on the fly's eye lens array **220** as the axially aligned rays passing through the focus **60**. This is because the fly's eye lens array **220** is located coincident with the concave image of the reflector formed by the field lens **210**. Because both the axially aligned rays **1, 2, 3, 4, 5, 6, 7, 8, 9**, and **10**, and the displaced rays **111, 12, 13, 14, 15, 16, 17, 18, 19**, and **110**, are reflected from the same points **2001, 2002, 2003, 2004, 2005, 2006, 2007, 2008, 2009**, and **2010**, (shown in **Figure 4**) on the primary reflector **200**, and since these points **2001, 2002, 2003, 2004, 2005, 2006, 2007, 2008, 2009**, and **2010**, are imaged onto the fly's eye lens array **220**, it follows that the on-axis rays **1, 2, 3, 4, 5, 6, 7, 8, 9**, and **10**, and the off-axis rays **111, 12, 13, 14, 15, 16, 17, 18, 19**, and **110**, come to the same points on the fly's eye lens array **220**.

[0087] **Figure 5** shows also that the image of the reflector **200** formed on the fly's eye lens array **220** has a sharp, well defined perimeter. The edge of the fly's eye lens array **220** is set to coincide with this sharply defined perimeter, so that essentially all the sunlight entering the receiver **70** is captured by the fly's eye lens array **220**.

[0088] An important role played by the field lens **210** in this invention is in forming a first, intermediate stage of concentration, and is illustrated by **Figure 5**. Practical generating systems should tolerate pointing misalignment that may arise from gravitational flexure and wind buffeting, as well as optical manufacturing and alignment errors that displace rays from

the ideal geometric design. In the present invention, the pupil image formed by the field lens **210** provides this tolerance, because equal division of first stage concentrated sunlight falling on the lenses of the fly's eye lens array **220** remains to a large degree also unchanged when the generator is mispointed slightly from the sun, thus the division of first stage concentrated sunlight is insensitive to mispointing.

[0089] The average intensity concentration factor at this first stage of concentration is equal to the ratio of the area of the reflector **200** to the area of the fly's eye lens array **220**. A typical value for this first concentration might be a factor 25, though this factor can range from 10 to 100 and still fall within the scope of this invention. In detail, the concentration after the first stage is higher in regions of the pupil away from the parent axis 50, for example at the lenses **221** and **222**. These lenses are made smaller, so all lenses receiver the same power. Conversely, the concentration after the first stage is lower in regions of the pupil close to the parent axis 50, for example at the lenses **224** and **225**. These lenses are made larger to receive the same power.

[0090] The second stage of concentration of the sunlight onto the individual cells **301, 302, 303, 304**, and **305**, is accomplished by the individual lenses **221, 222, 223, 224** and **225** of the fly's eye lens array **220.** These focus the already first stage-concentrated sunlight and further concentrate it onto the much smaller area of the cell **301, 302, 303, 304**, and **305**, respectively, behind each individual lens **221, 222, 223, 224** and **225**. Referring again to **Figure 5**, the fly's eye lens array **220** is shown in this example as five individual lenses **221, 222, 223, 224** and **225** focusing light onto cells **301, 302, 303, 304** and **305**, respectively. The geometric intensity concentration factor for this second stage of concentration, for each of the cells **301, 302, 303, 304** and **305**, is equal to the ratio of the individual lens area of the individual lenses **221, 222, 223, 224** and **225**, to the cell area. A typical value for this second concentration might also be 25, though this factor might again range from 10 to 100 and still fall within the scope of this invention.

[0091] The end-to-end geometric concentration, defined as the ratio of the area of entering sunlight that is focused onto a given cell **301, 302, 303, 304** or **305**, to the area of that cell, is the product of the concentrations in the first and second stages of concentration. This might typically be 25 x 25 = 625, but smaller or larger values, ranging from 100 to over 1000 could be readily achieved, and would fall within the scope of this invention.

[0092] Each PV cell **301, 302, 303, 304** and **305**, is centered on the axis of the individual lens **221, 222, 223, 224** and **225**, respectively, ahead of it. Thus, rays passing through

individual lens **221** are concentrated and focused onto cell **301**; rays passing through individual lens **222** are concentrated and focused onto cell **302**; rays passing through individual lens **223** are concentrated and focused onto cell **303**; rays passing through individual lens **224** are concentrated and focused onto cell **304**; and rays passing through individual lens **225** are concentrated and focused onto cell **305**.

[0093] Referring again to **Figure 5**, it will be seen that for the case of no mispointing, the rays (shown as solid lines in **Figure 4** and **Figure 5**) enter parallel to the paraboloid axis **50** and are focused at the centers of each of the cells **300, 301, 302, 303, 304**, and **305**. When the system is mispointed, the rays (shown as dashed lines in **Figure 4** and **Figure 5**) come to a focus displaced to the left edge of the cells **300, 301, 302, 303, 304**, and **305**. Rays from the range of angles representing the full disc of the sun will form images of the sun centered around the focus points shown in **Figure 5**.

[0094] **Figure 5a** shows in detail how the displacement of rays at the cells for a given mispointing angle may be equalized for all cells by varying the focal lengths of the lenses of the array **220** in proportion to their size. Thus the largest lens **225**, nearest the parent axis **50**, is made with the longest focal length **2255**, while the smallest lens **221**, furthest from the parent axis **50** has the smallest focal length **2215**. In this way, the distance between the on-axis focus **2250** and the mispointed ray focus **2251** of the lens **225** is made equal to the corresponding distance between the on-axis focus **2210** and the mispointed ray focus **2211** of the lens **221**. Such balancing of the image scale will be made for all lenses of the array, to ensure that the entire receiver **70** has uniform response to mispointing.

[0095] **Figure 6** shows from the viewpoint of the field lens **220** a detail of the same example of on-axis and off-axis focusing by adjacent approximately square individual lenses **223** and **224** of a fly's eye array **220**. The square cells **303** and **304** are centered behind each cell's associated individual lens **223** and **224**, respectively. In **Figure 6**, the illumination is modeled for the full disc of the sun, and the individual lens **223** and **224**, respectively, form images of the sun on each cell **303** and **304**, respectively.

[0096] Referring to **Figure 6**, for the on-axis case (no pointing error), the sunlight transmitted by individual lens **223** is concentrated in the solar disc image **3030** formed at the center of the cell **303**. Similarly, for the on-axis case, the sunlight transmitted by individual lens **224** forms a solar image **3040** centered on the cell **304**. For the off-axis case (mispointing error), the sunlight transmitted by individual lens **223** forms a displaced solar

image **3031** on the cell **303**, and the sunlight transmitted by individual lens **224** forms a displaced solar image **3041** on the cell **304**.

[0097] As modeled here and for the example shown in **Figure 6**, the square cells **303** and **304** are one fifth the size of the square individual lenses **223** and **224** used in the fly's eye lens array **220**. It follows that the average second stage geometric intensity concentration factor, given by the ratio of the area of an individual lens **223** to the area of the associated cell **303**, is 25 for purposes of the present invention.

[0098] **Figure 6** may be used to describe and illustrate two potential limitations that arise with the type of second stage concentration discussed so far. One is that the local intensity concentration of sunlight is much higher than the average second stage concentration, because the sunlight is concentrated in the sun's image which covers only a fraction of the area of each cell **303** or **304**, which are shown as examples in **Figure 6**. To handle such high local concentration, CPV cells have been made specially with widened surface conductors, but such CPV cells do not convert incident light power into electrical power with as high efficiency as other types of PV cells optimized for the lower concentration typically distributed across most of the cell area of a typical PV cell.

[0099] The second limitation is that of tolerance to mispointing. As shown in **Figure 6**, the effect of mispointing is to move the concentrated light **3031** or **3041**, to the edge of the cell **303** or **304**, respectively. For a mispointing angle any larger than the example illustrated in **Figure 6**, some concentrated sunlight will move off the cell **303** or **304** and be lost, lowering the conversion efficiency.

[00100] These limitations may be mitigated by incorporating a dome lens **233** placed in contact with each associated cell **301**, **302**, **303**, **304**, and **305**. Such dome lenses **233** have sometimes been used in conventional concentrating PV systems to mitigate chromatic aberration of Fresnel lenses, (something which is much reduced in this invention), as well to improve light distribution across a PV cell.

[00101] **Figure 7a** and **Figure 7b** show in a preferred embodiment a comparison in which a dome lens **233** is introduced, as shown in **Figure 7b**, to increase tolerance to mispointing angle and to more uniformly illuminate an associated cell **303**. **Figure 7a** illustrates an example without a dome lens **233**. **Figure 7a** shows on-axis rays, two of which are identified with reference numerals **51** and **61**, entering an individual lens **223** of the fly's eye array **220**, and which on-axis rays **51** and **61** are brought to a focus **75** centered on the cell **303**. In addition, two parallel rays **161** and **151** that are at a relatively large off-axis angle are brought

to a focus **76** that lies above (as shown in **Figure 7a**) and outside the cell **303**. These off-axis rays **161** and **151** would thus generate little or no electricity in the cell **303** in the illustrated example. **Figure 7c** also shows a magnified plan view of the cell **303** shown in **Figure 7a**, illustrating in more detail the same central and vertically displaced foci **75** and **76**.

[00102] **Figure 7b** shows the same on-axis and off-axis rays refracted by the individual lens **223** of the fly's eye lens array **220** and coming to the same foci **75** and **76** as in **Figure 7a**, but now with the addition of a dome lens **233** in contact with the cell **303**. The lens is preferably placed with its entrance surface **2330** centered on the focus **75**, and is preferably large enough to intercept also the off-axis rays, (for example rays **151** and **161**), focused at **76**. Now after refraction upon passing into the dome lens **233**, all the rays (for example rays **51**, **61**, **151** and **161**), both on-axis rays **51** and **61**, and off-axis rays **151** and **161**, fall on the cell **303**. The addition of the dome lens **233** thus provides substantially greater tolerance to mispointing angle. **Figure 7d** shows a magnified plan view of the photovoltaic cell **303** shown in **Figure 7b**, illustrating in more detail the focus of sunlight for on-axis rays **51** and **61**, and the focus of sunlight for off-axis rays **151** and **161**, in the example shown in **Figure 7b** illustrating the effects of mispointing with a dome lens **233**. Referring to **Figure 7d**, the dome lens **233** also provides more uniform illumination and eliminates the high local concentration, which is shown in **Figure 7c** without the dome lens **233**. Refraction by the front surface of the dome lens **233** acts to form an image of the individual lens **223** on the cell **303**.

[00103] In a presently preferred embodiment, the optimum shape for each individual lens element **221, 222, 223, 224** and **225** of the fly's eye lens array **220** is square, since each of their images is then also square, and the associated image of each individual lens element **221, 222, 223, 224** and **225** will be most uniformly spread across the associated square multijunction cell **301, 302, 303, 304**, and **305**, respectively. It follows that the primary reflector **200** is preferably square (or rectangular), so that the corresponding approximately square (or rectangular) pupil image formed by the field lens **210** is tiled by an array of contiguous individual lenses (for example individual lenses **221, 222, 223, 224** and 225) in the fly's eye lens array **220** that individually are also approximately square (or rectangular). It follows that the exit pupils are also approximately square (or rectangular), and are readily divided into an array of approximately square individual lenses (for example individual lenses **221, 222, 223, 224** and **225**) in the fly's eye array **220**, that are imaged by the dome

lens **233** to match the shape of the square multijunction cells (for example, the square multijunction cells **301**, **302**, **303**, **304**, and **305**, respectively).

[00104] **Figure 7e** shows the same on-axis and off-axis rays refracted by the individual lens **223** of the fly's eye lens array **220** and coming to the same foci **75** and **76** as shown in **Figure 7a**, but now with the addition of an optical reflecting funnel **253** in optical contact with the cell **303**. The funnel **253** is preferably made of glass, such as fused quartz, with the rays undergoing total reflection, and the entrance face antireflection coated. The funnel **253** is preferably placed with its entrance surface **2530** centered on the focus **75**, and large enough to intercept also the off-axis rays (for example rays **151** and **161**) focused at **76**. The exit surface **2531** of the funnel **253** is preferably the same shape as and in optical contact with the cell **303**. Now after one or more reflections on the walls **2532** of the funnel **253**, all the rays, both on-axis rays **51** and **61** and off-axis rays **151** and **161**, are reflected onto the cell **303**. The addition of the optical funnel **253** thus provides substantially greater tolerance to mispointing angle. **Figure 7f** shows a magnified plan view of the photovoltaic cell **303** shown in **Figure 7e**, illustrating in more detail the rays of sunlight striking the cell **303** for on-axis rays such as **51** and **61**, and off-axis rays such as **151** and **161,** illustrating the effects of mispointing. The rays are scattered across the cell **303**, thus the funnel **253** provides more uniform illumination of the cell **303** and eliminates the high local concentration, as compared to that shown in **Figure 7c** without the funnel **253**.

[00105] **Figure 8a** shows schematically a side cut-away view of a single cell **303** with a dome lens **233** in an example of a cooling configuration for use in an embodiment of the present invention. **Figure 8b** shows schematically a side cut-away view of a single cell **303** with a dome lens **233** in a different example of a cooling configuration for use in an alternative embodiment of the present invention. The electrical connection in both configurations is made to the underside of the cell **303** is made through the copper land **433** attached to a ceramic circuit card **413**. The electrical connection to the upper side of the cell **303** is made via wire bonds to the copper land **423**. Terminals on lands **423** and **433** are used to connect the cell **303** to other cells (for example, cells **301**, **302**, **304**, and **305**) in the array of cells to form the electrical output of the receiver **70**.

[00106] **Figure 8a** shows also how in the illustrated embodiment the heat generated in a cell **303** may be removed by conduction and forced convection. Heat generated by the cell **303** is conducted through the copper land **433** and the ceramic card **413** via a thermally conducting bond **483** to a thermally conductive support **443** behind, aluminum or copper

being preferred materials. In one preferred embodiment, the full array of cells **300** mounted on plates such as **443** may be supported in position behind the fly's eye lens array **220** by a concave meniscus or bowl **450**. Heat may be transferred via thermal grease, gel or adhesive from the conductive cell support **443** through the bowl **450** to a heat sink **463**. It should be understood by those familiar in the art that the bowl **450** will distribute heat laterally by thermal conduction, and that the finned heat sink elements **463** need not register precisely with the cells, as shown in **Figure 8a**

[00107] In the embodiment shown in **Figure 8a**, the side openings of the heat sink **463** are partially blocked by sheets **473** on either side, and air is forced upward, as shown by arrows in **Figure 8a**, to exit through gaps near the bowl **450**. By configuring in this way for forced air convection through an array of heat sinks **460**, all of the cells of the cell array **300** may be cooled. For example, if the first stage concentration of sunlight entering the fly's eye lens array **220** is 25x, and the cells **300** convert half to electricity and half to heat, the average heat density at the bowl **450** for a clear-day incoming solar flux of 1000W/m^2 is approximately 12,000 W/m^2.

[00108] The heat sink **463** is preferably designed so that the total surface area of its fins **466** under forced air convection is approximately 20 times that of the area of the face **464** of the heat sink in thermal contact with the bowl **450**. Thus the cooling at this face is 20 times greater than the typical cooling coefficient of 50W/m^2/°C for forced convection, *i.e.*, 1,000W/m^2/°C. For dissipation of 12,000 W/m^2, the heat sink fins would thus run 12°C above ambient temperature. Taking into account the conduction thermal gradients, we can expect the temperature of the bowl **450** to run around 20°C above ambient, which provides very good cooling.

[00109] **Figure 8b** illustrates an alternative embodiment using an alternative method of cooling in which a thermal transfer liquid **490** is constrained by a sealed element **491** to flow behind and to be in intimate thermal contact with the bowl **450**. In this way the heat from the cells **300**, (for example cell **303** shown in **Figure 8b**), may be removed and harvested as an additional form of energy from the generator. It will be understood by those familiar in the art that many forms of flow manifolds might be used to remove the heat while remaining within the scope of this invention.

[00110] **Preferred embodiments of the receiver with high throughput optics**

[00111] In order to realize the full potential for high overall efficiency of conversion of sunlight into electricity, in highly preferred embodiments of the invention, the refractive

optical elements of the receiver **70** are optimized for maximum throughput to the cells **300**, by minimizing losses by absorption and from surface reflections.

[00112] **Figure 9** shows schematically the reflection losses in the receiver optics, namely the field lens **210**, the fly's eye lens array **220**, and one of the dome lenses **233**, that are addressed in these embodiments. Following the path of a typical ray **519**, on entering the field lens **210**, some of the power in ray **519** is lost to reflection from the entrance surface **2330**, shown as ray **511**. Let the fraction of power lost be r_f. The same fraction is lost again in the reflected ray **512** at the second surface of the lens. In addition, some light will be lost to absorption by the glass material, with a fraction t_f transmitted. Thus the intensity of the ray **513** exiting from the field lens **210** will be reduced by the following factor

[00113] $$t_f(1-r_f)^2.$$

[00114] Similar reflection losses take place as ray **513** transmitted by the field lens **210** passes through the fly's eye lens **223**, with a fraction "r_g" lost to each of the surface reflected rays **514** and **515**. Additional loss takes place by absorption when the transmission "t_g" of the lens **223** is less than 1. Finally, the ray **516** exiting the fly's eye lens **223** will lose also a fraction "r_g" in the ray **517** reflected at the surface of the dome lens **233**. The gap between the lens **233** and the cell **303** is preferably filled with index matching optical adhesive, avoiding further surface reflection loss. The transmission of the dome lens **233** is taken to be "t_s." In all, accounting for all the reflection and absorption losses, the typical ray **519** that enters the cell **303** as ray **518** is reduced in intensity by the following factor

[00115] $$t_f t_g t_s (1-r_f)^2 (1-r_g)^3.$$

[00116] For purposes of explanation, only one example ray **519** has been described in detail. Persons skilled in the art, having the benefit of this description, will appreciate that all rays reflected by the primary mirror **200** will suffer similar losses.

[00117] An additional loss of light received by the cells **300** takes place at the quilted entry surface **250** of the fly's eye lens array **220** if the boundaries between the individual lenses (for example individual lenses **221, 222, 223, 224** and **225**) are imperfectly formed. **Figure 9** illustrates this loss in the boundary region **2232** between individual lenses **223** and **222** which is imperfectly formed; and over width "w" the boundary region **2232** does not direct entering rays to either of cell **303**, or adjacent cell **302** (not shown in **Figure 9**). The correctly formed region **2231** of the individual lens **223** has width "s". With these dimensions, the added fractional loss due to scattering at the edges of the individual lenses is

$2w/s$, and the total receiver throughput "T", taking into account losses from surface reflection, glass absorption and edge scattering, is:

[00118] $$T = (1-2w/s) \quad x \quad t_f t_1 t_2 \quad x \quad (1-r_f)^2(1-r_1)^3,$$

[00119] *(edge loss x total transmission loss x total reflection loss).*

[00120] While each component loss may be small, if not addressed they may together combine to an unacceptable total. For example, if each glass surface were uncoated, the reflection loss would be approximately 3.5%, *i.e.*, r=0.035. The total reflection loss would then be ~ 16%. If an additional 3% of the power were lost by absorption in each individual lens, *i.e.*, t = 0.97 for each individual lens, the total transmission loss will be 9%. To estimate the losses from imperfect formation of the fly's eye lens array **220**, we take as an example the case where loss between individual lenses of side length s=25 mm is over width w=0.5 mm; then edge loss will be 4%. Taking these reflection, transmission and edge losses all together, the total transmission "T" of the receiver would be an undesirably low 73%. Thus preferred embodiments of the present invention include features to minimize all three types of loss, as described more fully below.

[00121] In considering the requirements for minimizing transmission and surface reflection losses, it is important that these losses be low across the wide spectrum of solar radiation that is utilized by multijunction cells **300**. To reach their full conversion efficiency, the full range of this spectrum should be transmitted free of significant loss.

[00122] To minimize transmission loss in the field lens **210**, it is made preferably of fused silica. This material is preferred because it has negligible absorption (<0.1% through 10 cm thickness across the solar spectrum (400 – 1600 nm wavelength)). Such high transmission is important not only to avoid loss of efficiency, but also to avoid overheating of the field lens **210**. Thus for example, if the primary reflector **200** were to have area 10 m^2, the sunlight power passing through the field lens **210** would be as high as 10 kW, and 0.1% absorption would heat the lens **210** with 10W of power. From this amount of absorbed heat, there would be essentially no risk of thermal fracture, because fused silica has the additional advantage of very low thermal expansion.

[00123] To minimize surface reflection loss over the full bandwidth of the solar spectrum, in preferred embodiments of the invention, the fused silica field lens **210** is given an antireflection coating. Here we disclose an advanced coating process with double sol-gel layers that results in very low reflection loss over the very wide spectral bandwidth of multi-junction PV cells **300**.

[00124] The layers applied to both sides of the silica lens **210** consist solely of porous silica, with each layer having a different degree of porosity to differentiate the refractive indices. The two coating materials were selected to yield a bottom layer refractive index of 1.33-1.40 and a top layer refractive index of 1.17-1.25. The thicknesses of each layer were optimized for the entire solar spectrum range (400nm - 1800nm). In the past, double layer porous silica coatings have been applied to fused silica for high powered lasers (Sun, Yingying "SiO2-ORMOSIL Double-layered broadband antireflective coating for high powered lasers", 2016), and PV glass (Liping, Zou "An Abrasion Resistant and Broadband Antireflective Silica Coating by Block Polymer Assisted Sol-Gel Method", 2013).

[00125] The method described here differs in the thicknesses and indices of the two porous layers, which are tailored for broad band antireflection across two full octaves of the solar spectrum (400 – 1600 nm wavelength) rather than two specific wavelengths of Sun, Yingying (532 and 1064 nm). Also, the process disclosed herein using spin coating and very high temperature firings is designed specifically to produce very robust coatings that will stand up to many years of exposure outdoors.

[00126] **Figure 10a** shows schematically a spin coating apparatus designed to fit the geometry of the field lens **210**. The sol is dispensed onto the lens **210** by the syringe **2101**. The lens is carried by the spinning bowl **2102**, driven by the motor **2103**. The two layers are applied in separate steps and are derived from two different solutions of suspended silica particles yielding different microstructures of silica upon deposition. The concentrations of these solutions are between 1-5%. Depending on the concentration, the spin rates used for deposition will be between 500-1500 RPM. Each layer is fired separately at a high temperature in order to consolidate into a very robust layer. The firing temperatures lie in the temperature range 500-900 C maintained over 1-3 hours.

[00127] **Figure 10b** shows the measured reflectivity of a coating on fused silica obtained according to the antireflective coating process disclosed herein. The solid line shows the measured reflectivity of a single surface; where the measurement shown in **Figure 10** b was made from 400 nm wavelength to about 1000 nm wavelength. The small circles show the calculated reflectivity, which was calculated beyond the range that was measured, and was calculated out to 1600 nm wavelength.

[00128] In preferred embodiments of this invention, the additional lenses within the receiver, namely the fly's eye lens array **220** and the dome lenses **233,** have aspheric surfaces, and made preferably at low cost from molded or hot-pressed glass. In a preferred

embodiment, this glass is a low-expansion type, such as low-expansion borosilicate glass, to provide tolerance to thermal stress. Hot pressed lenses of such glass are made by industry in high volume, for high power illumination systems for example. For application in this invention, low-expansion borosilicate glass has a major advantage, in that it may be given an antireflection surface treatment with extremely low reflectivity over a very broad spectral range by a thermal and chemical process, as disclosed herein, in a simple, inexpensive process.

[00129] The process involves heat treating the molded borosilicate lens at temperatures between 570 - 650°C for 6-24 hours to induce phase separation in which a silica rich phase and an alkali-borate rich phase is formed in equilibrium with one another. The lens is then placed into an etch bath consisting of 5-15% solution of ammonium bifluoride for 10-60 minutes to remove the skin layer formed during hot pressed molding, which tends to be silica rich, and to expose the phase separated material beneath. The lens is then leached with a mineral acid at 20-25% concentration for 5-20 minutes. Usable acids include sulfuric, nitric, phosphoric, and fluorosilicic.

[00130] Figure 11 shows the exceptionally low reflectivity over very wide spectral range realized by this process. The glass treated here was a 200-micron thick MEMpax borosilicate cover slide, which was heat treated at 600°C for 24 hours. The glass was then leached in a 10% solution of ammonium bifluoride for 15 minutes, followed by a 10 minute leach at 45°C in a solution containing 25% fluorosilicic acid, 1.5% ammonium bifluoride, and the balance distilled water.

[00131] A suitable process of phase separation and leaching for reducing surface reflectivity is described by (Pettit, Richard. "Antireflection Pyrex Envelopes for Parabolic Solar Collectors", 1983) and (Haggerty, John S. "MIT Energy Laboratory Report No. MIT-EL 82-016", 1982). The process disclosed herein is distinct in its application to press molded lenses of glass with very low absorption and unusual geometry. This process was originally designed for use with Corning 7740 Pyrex. MIT Energy Laboratory Report No. MIT-EL 82-016 explored the use of a soda-lime glass with an 80/10/10 composition of $SiO_2/Na_2O/CaO$ for use with float glass. Different compositions of glass will require different heat treatment schedules to achieve the desired spinodal microstructure of phase separation.

[00132] The composition of glass for the lenses of this invention will preferably have very low iron content, lower than found in commercially available borosilicate glasses. Typical borosilicate glasses are made for very high transmission in visible wavelengths of

light, but for the present invention, typical borosilicate glasses have significant iron absorption at longer wavelengths in the near infrared, where solar emission is still strong, and that is a drawback for the present invention.

[00133] **Figure 12** shows the spectral energy distribution of sunlight (standard spectrum AM 1.5 shown by line **253)** as a function of wavelength up to 2000 nm, together with the fractional absorption of light, (1-t), on passage through 19 mm thick borosilicate glass of a widely used commercial type (Schott Borofloat) (shown by line **252**). 19 mm thickness is representative of the combined thickness of the fly's eye lenses **220** and the dome lenses **233** of preferred embodiments of this invention, and thus of the absorption loss we could expect if both the fly's eye lens array **220** and the dome lens **233** were made of borosilicate glass of this composition. The absorption line **252** shows the percentage absorption as a function of wavelength of the sunlight for the specified borosilicate glass. The line **253** shows the energy distribution of sunlight as a function of wavelength of the sunlight, representing a standard AM 1.5 spectrum.

[00134] The absorption averages around 5% across the solar spectrum from 400 to 2000 nm wavelength, with a broad peak of around 8% at around 1100 nm wavelength. This peak is due to a ferrous iron impurity of around 200 ppm. For this invention, in which the sunlight in converted into electricity by multijunction PV cells **300**, absorption of wavelengths between around 950 nm and 1600 nm, which fall into a single junction, may cause a proportional drop in the power output of the cell **303**, *i.e.*, around 6%. For the molded borosilicate fly's eye lens array **220** and the dome lens **233** of this invention, the absorption would preferably be an order of magnitude less, with the ferrous iron content ideally less than or around 20 ppm.

[00135] **Methods of manufacture of the fly's eye lens array**

[00136] In preferred embodiments of this invention, the fly's eye lens array **220** may contain a large number of individual lens elements. The representative array illustrated in **Figure 3** might be used in a 1 kW receiver as the second stage of concentration powering a 12 x 12 array of multijunction cells **300**. As indicated, a preferred material for the fly's eye lens array **220** is low-expansion borosilicate glass, molded or hot pressed to form the aspheric surfaces of each lens element of the array **220,** but the methods of manufacture are applicable to other glasses with other advantages, such as lower molding temperature.

[00137] As discussed above, preferred methods of manufacture of the fly's eye lens array **220** will minimize the loss of light due to any imperfections in the formation of the quilted

entry surface **250** of the lens array **220**. Here we disclose alternative methods of manufacture aimed at reducing such loss to less than 1%, *i.e.*, w/s < 1/200. In method 1 lenses are first individually molded, typically round, to the required focal length(s), then cut to form the different size and approximately square individual lens elements to be mechanically assembled together into the fly's eye lens array **220**. In method 2, a plurality of elements are molded in one step either as a complete fly's eye lens array **220** in a single piece**,** or as sub-arrays to be fitted with other sub-arrays to form the complete fly's eye lens array **220**.

[00138] **Method 1 - Mosaic assembly**

[00139] **Figure 13a** shows a lens **22** with convex aspheric upper surface **2231**. A plurality of lenses **22** are press-molded and subsequently phase separated by holding at appropriate temperature, as described above. **Figure 13b** shows a single lens **223** made by cutting a lens **22** to the correct shape to fit as an element of the fly's eye lens array **220**. The cut sides are preferably angled as shown, so a plurality of lens segments **223** will fit closely together to form the fly's eye lens array **220**. The individual press-molded lenses are cut accurately into the individual, differently-shaped segments needed to form said array with minimal gaps.

[00140] Referring to **Figure 9**, in order to minimize the boundary region **2232**, the cut made on the molded aspheric side **2231** of the lens must be accurate and clean to the edges. A preferred method of cutting is by water jet. In a preferred procedure, the water jet enters on the lower side **2233** shown in **Figure 13b** and exits the more curved side **2231**, to eliminate surface roughness on the edges of the cut due to spreading of the water jet before impact. Such roughness on the side **2233** of the lens **223** is not a problem, because on entering the lens **223**, the light is refracted away from the cut edge, as shown in **Figure 7**. In another preferred method, the lenses may be cut using a diamond saw.

[00141] To build up sub-arrays or the full fly's eye lens array **220**, the cut sides of the mosaic lens elements **223** may be glued together. Preferably, the glue is wicked in from the side **2233** shown in **Figure 13b**, so as to avoid an accumulation forming a boundary region **2232** (as illustrated in **Figure 9**) from the glue itself.

[00142] Referring to **Figure 13c**, as an alternative or in addition to side gluing, the individual lens elements **223** may held in position to form the full fly's eye lens array **220** by optical bonding the faces **2223**, **2233** and **2243** to a faceted glass bowl. In this method, the leaching process to produce the antireflection property is preferably carried out after the subarrays or full fly's eye lens array **220** is assembled, to minimize handling that could damage the coated lens surfaces **2231**.

[00143] Referring to **Figure 13d, Figure 13e and Figure 13f**, the full fly's eye lens array **220** may be assembled alternatively from the cut lens elements by bonding them individually to an underlying supporting structure, constructed with openings so as to avoid light blocking. **Figure 13d** shows schematically such a supporting structure **900** made in the style of a slotted egg crate. Component elements are slotted arcs, as shown in **Figure 13e**, made for example from laser-cut aluminum sheet. Arc **911** has cut into it the five slots **9111, 9112, 9113, 9114** and **9115**, while arc **921** has slots **9211, 9212, 9213, 9214** and **9215**. The slots are parallel to each other. In **Figure 13d**, the five slotted arcs **911, 912, 913, 914** and **915** slot over the five arcs **921, 922, 923, 924** and **925**, making a structure to carry 36 individual lenses in a 6x6 array. It should be understood that **Figure 13d** is a schematic diagram, and the number and shape of the arcs will be chosen to match the desired fly's eye array. In general, the arc shapes and slot positions will be different for every arc, so that every cell of the structure **900** matches precisely the dimensions of the fly's eye lens array.

[00144] The upper surfaces of all the arcs, such as **9110** and **9210** in **Figure 13e,** in the full assembly **900** will be constructed so that they define the desired shape of the fly's eye lens array. Each cell is the size needed to match the size of the lens to be attached. Referring to **Figure 13f**, the upper surfaces of the arcs **912** and **922,** here shown in detail, may be provided with locating tabs such as **9121** and **9221,** and the lenses with slots such as **2331** and **2332**, sized and positioned to ensure accurate registration of each lens **233** to its cell **303**. Thus slot **2331** in lens **233** engages with slot **9121**, and slot **2332** engages with tab **9221**. The slotted arcs **911** and **921** will preferably be made thin enough so as to not block light refracted by the lens elements to the multiple foci. **Figure 13g** illustrates how incoming rays **51** and **61**, upon refraction at the upper surfaces of the lenses **222, 223** and **234**, are refracted toward the lens focus and away from the arc segments **912** and **922**, and are not blocked by the arcs **911** and **912** of the supporting structure.

[00145] **Method 2 - Molded array**

[00146] In an alternative molded array method, the entry surfaces of a plurality of adjacent elements of the fly's eye lens array **220** are formed together by hot-pressing glass against a quilted mold. Those familiar with the art will appreciate that while hot pressing is a well-established process for forming complex decorative patterns in glass bowls, for example with the appearance of cut glass, the very sharply defined boundaries desirable in accordance with the present invention have not been achieved in large arrays of molded lenses.

[00147] **Figure 14a**, **Figure 14b** and **Figure 14c** show schematic diagrams of steps in a preferred embodiment of an alternative process to realize sharp definition. Referring to **Figure 14a**, the first part of the mold **800** is quilted with the inverse shape of the desired fly's eye lens array **220** or subarray, and is overall convex in shape. The second part of the mold **810** is concave with grooves **840** to take the glass squeeze-out, cut radially, as shown in **Figure 14b**. The glass preform **820** may take the form of a plate of uniform thickness, as shown in **Figure 14a**, or of a plurality of individual gobs. To mold the glass **820**, both the first part **800** and the second part **810** of the mold, and the glass preform **820**, are all first brought to the same temperature, which is the temperature needed to soften the glass **820**. Pressure is then applied to form the quilted side of the glass array in an essentially isothermal process. During this process to form the first surface of the fly's eye lens array **220**, excess glass **821** may be squeezed out around the perimeter of the mold **810** and also into the radial grooves **840** in the second part **810** of the mold. By holding the mold **800** and **810** and the glass **820** close to isothermal during the pressing, there is little lateral stress from differential expansion between the glass **820** and the mold **800** and **810**, and thus wear on the sharp features of the mold **800** is minimized, to maximize longevity.

[00148] On completion of the formation, with the quilted first surface **250** of the glass correctly formed, the first part of the mold **800** is parted while still at the molding temperature, ready to form the next array. **Figure 14c** shows the just-formed and still relatively soft molded glass **822**, supported by the concave second lower side of the mold **810**. In the next step, the now molded glass **822** and the second part of the mold **810** are cooled to freeze the glass **822**. During this cooling, radial groves **840** may be incorporated to allow for differential expansion of the squeezed-out glass **821** with minimal wear between the support **810** and the glass **822**. Once the temperature has reached that needed for phase separation, the molded glass **822** may be held at that temperature until phase separation is completed. The glass **822** so formed with the array of lenses on the first side **250** may be cut around the edges and ground and polished on the second surface **823** to remove any squeezed-out features.

[00149] **Specific designs of two preferred first stage concentrators**

[00150] **Figure 15a** shows a ray trace diagram for a specific preferred example design of a first stage concentrator. The prescription for this example is given in **Table 1**.

[00151] The paraboloidal mirror **200** had a 2.5 m focal length. The entrance aperture of the paraboloidal mirror **200** was square, 3.3 m x 3.3 m, and was offset 1.7 m from the

paraboloid axis **50**. In this example, the ray trace diagram in **Figure 15a** was generated as an illustrative example. The detail of **Figure 15b** shows the field lens **210** which was a meniscus of fused silica positioned 50 mm beyond the paraboloid focus **60**. The lens **210** formed a pupil image with radius of curvature 0.7 m.

[00152] For the example described in connection with **Figure 15b**, a footprint plan view of the first stage concentration pupil image is shown in **Figure 16**, within a 0.76 m square outline. The concentration averages 20x. The crosses depicted in **Figure 16** show the position in the pupil of five sets of parallel rays entering on a uniform grid, on-axis and ± 0.5° off-axis, in both azimuth and elevation. A fly's eye lens array **220** according to this invention, whose individual lens corners coincide with the grid of points in this **Figure 16**, will divide the sunlight in the pupil image into equal amounts, independent of small mispointing errors.

[00153] **Figure 17a** and **Figure 17b** show a preferred embodiment of a solar generator according to the present invention configured to be balanced about both the elevation axis **151** and azimuth axis **161**. Balanced systems may be preferred because of their potential for lighter weight and lower cost tracking.

[00154] **Figure 17a** shows a plan view of the generator incorporating two off-axis paraboloidal reflectors **201** and **202** and their respective fly's eye receivers **722** and **72**. Their respective paraboloid axes **53** and **52** are vertical, marked as small circles. The receivers **722** and **72** are adjacent to each other and positioned between and facing to the centers of the associated reflectors **201** and **202**, respectively.

[00155] **Figure 17b** shows a side view of the generator **1000** illustrated in **Figure 17a**. Sunlight rays **1**, **2** and **3** incident of reflector **201** are focused into receiver **722**; while sunlight rays **4, 5** and **6** are directed into receiver **72**.

[00156] The elevation structure **500** comprises an integrated lightweight structure **540** supporting both reflectors **201** and **202** and rigidly connected to the lightweight vertical structure **530** that carries both receivers **722** and **72**. The elevation bearing **150** is positioned so that its axis **151** passes through the center of gravity of the elevation structure **500**. The elevation bearing **150** is supported by an azimuth bearing **160** atop a fixed post **170**. As shown in **Figure 17b**, the elevation structure **500** is relieved on the side in front of the post **170**, so it is free to tilt downward in elevation, when the receivers **722** and **72** move out toward the viewer. Forced convective cooling of the receiver **72** is provided by an axial fan **727**. A similar axial fan is provided for the receiver **722**.

[00157] **Figure 18** is a plan view of a second preferred embodiment of the invention, a generator **1000** with two adjacent large square off-axis paraboloidal reflectors **201** and **202.** Sunlight rays striking the first reflector **201,** are focused into a first receiver **722**, where they are converted into electricity. Similarly rays striking the second reflector **202** are focused into a second receiver **72**. The first and second receivers **722** and **72** are fixed in position relative to the first and second reflectors **201** and **202**, respectively, by arms positioned below any incoming rays to receive all reflected rays (not shown, but similar to **531** and **532** in **Figure 1).** In this preferred embodiment, the primary reflectors **201** and **202** are positioned adjacent to each other, with no significant gap. Their parent axes **50** and **51** (vertical in this plan view and therefore shown as dots) are offset in the y direction but are symmetric to each mirror in the x direction.

[00158] **Figure 19** shows a ray trace diagram for this second preferred embodiment, whose optical prescription is given in **Table 2**. In this example, the paraboloidal mirror **200** has a 3 m focal length. The entrance aperture of the paraboloidal mirror **200** is square, 3.17m x 3.15m, and is offset 1.7 m from the paraboloid axis **50**. **Figure 20** shows in more detail a ray trace of the field lens **210,** a meniscus of fused silica positioned 90 mm beyond the paraboloid focus **60**. The lens **210** weighs 1.52 kg and forms a pupil image on the curved surface **2220**, where the fly's eye lens **220** (not shown) will be located.

[00159] A footprint plan view of the first stage concentration pupil image on the surface **2220** is shown in **Figure 21,** with a 0.6 m square outline shown for scale. The concentration averages 28x. The point clusters depicted in **Figure 21** show how parallel rays of light in a uniform grid that enter the primary mirror **200** are brought to a focus on the surface **2220**. The grid of 22 x 22 ray bundles shown marks the position of rays that enter the system on-axis and ± 0.75° off-axis in both azimuth and elevation. A fly's eye lens **220** in a 22 x 22 array, according to this preferred second embodiment of the invention, placed with the corners of the individual lenses coincident with the grid points in **Figure 21**, will divide the sunlight in the pupil image into a 22 x 22 array of equal amounts, largely independent of small mispointing errors.

[00160] **Figure 22** and **Figure 23** show a preferred embodiment of a dual axis tracker according to this invention. The tracker is designed for use both with essentially flat reflectors as a heliostat, as shown, or with dish-shaped reflectors with fly's eye receivers, as shown below in **Figure 25**. The tracker comprises a lower rigid spaceframe structure **400** that rotates on a circular ground track **310** about a lateral ground restraint **311,** and an upper

hinged elevation spaceframe **500** carrying solar reflectors **230** and driven about an approximately horizontal axis defined by nodes **501** and **502** by a linear actuator **600**. In operation, the solar reflectors are set to their desired orientation by a combination of driving the structure **400** around the track and setting the length of the actuator **600**.

[00161] The lower spaceframe **400** is supported on the track **310** by three wheels **406**, **407** and **408**, which are attached to nodes **403**, **404** and **405** that form the base triangle of the spaceframe **400**. One or more of these wheels is motorized, and used to rotate the structure **400**. The center of rotation is fixed by a lateral ground anchor **311**, to which is attached a central lowest node **409** of the structure **400**. The coupling to the anchor **311** is such as to constrain lateral motion, so that the wheels remain on the track, but not to constrain downward motion. In this way we ensure that the rigid spaceframe **400** is not over-constrained. Of the six degrees of freedom of rigid body motion, four are controlled by the rotation of the three wheels around the track (vertical position, tip, tilt and rotation), and lateral position (x and y) by the center ground anchor. Irregularities in the ground track will result in the "elevation" axis of rotation **501 -502** being not exactly horizontal, but this does not prevent accurate tracking as long as the orientation is known from calibration or closed loop servo. A combination of rotation about an axis within a few degrees of vertical and elevation can get to any orientation needed for heliostat tracking or sun pointing.

[00162] **Figure 24** shows a preferred embodiment of the lateral ground anchor and its connection to the lowest node **409** of the spaceframe structure, which connects via struts to the nodes **420**, **421** and **422** of the spaceframe **400**. The anchor **311** is a helical pier with the blade **314** deep in the ground **330**. At its upper end the shaft **311** passes through a bushing **315,** which may for example be of hard bearing plastic needing no oil, that transmits lateral forces from the node **409**. A concrete disc **316** then transmits these forces into the ground **330**. The node **409** is free to move vertically over the range needed to handle track irregularities, but in the event that a wind gust lifts one or more of the tracker wheels **406**, **407** and **408** off the track **310**, then further upward motion of the spaceframe structure **400** is prevented when the node **409** contacts the head **312** of the helical shaft **311**.

[00163] The rotation angle of the tracker structure **400** with respect to the fixed helical anchor **311** is measured by the angular encoder **410** attached to the node **409**. A top extension **313** of the helical anchor **311** provides the central angular reference. The bushing **315** and encoder **410** are protected from dirt by the cover **411** which form the central moving element of a labyrinth seal, with rings **317** and **318** forming the fixed elements.

[00164] **Figure 25** shows the same preferred embodiment as shown in **Figure 23** of a dual axis tracker according to this invention, except now adapted for two off-axis solar reflectors **201** and **202** powering fly's eye receivers **722** and **72**. The tracker comprises the same lower rigid spaceframe structure **400** on a circular ground track **310**, but in this embodiment the elevation spaceframe structure **500** is now extended out in front of the reflectors to nodes **5772** and **572**, which hold in position the receivers **772** and **72**. The nodes **5772** and **572** are connected by struts to the nodes **518, 519, 520** and **5212** that project below the lower edges of the reflectors **201** and **202**, and which in turn are connected through the spaceframe structure **500** to its primary nodes **501** and **502** that define the elevation axis, and **503** and **504** adjacent to the elevation drive **600**.

[00165] Those skilled in the art, after having the benefit of this disclosure, will appreciate that modifications and changes may be made to the embodiments described herein, different design parameters and materials may be substituted, equivalent features may be used, changes may be made in the assembly, and additional elements and steps may be added, all without departing from the scope and spirit of the invention. This disclosure has set forth certain presently preferred embodiments and examples only, and no attempt has been made to describe every variation and embodiment that is encompassed within the scope of the present invention. The scope of the invention is therefore defined by the claims appended hereto, and it is not limited to the specific examples set forth in the above description.

TABLE 1 Optical prescription for a preferred example of the first stage concentrator

	Surface type	Radius (mm)	Thickness (mm)	conic
1	Mirror (**200**)	-5000	-2550	-1
2	Silica (lens **210** entrance)	400	-30	0
3	Air (lens **210** exit)	155	-700	0
4	Image (coincident with lens array **220**)	700	-	0

TABLE 2 Optical prescription for a second preferred example of the first stage concentrator

#	Radius	Thickness	Material	Semi-Diameter	Conic	Decenter Y	Tilt About X
0	Infinity	Infinity		0.000	0.000	0.000	0.000
1	Infinity	5000.000		5065.454	0.000	0.000	0.000
2	-6000.000	-3000.000	MIRROR	5027.574	-1.000	0.000	0.000
3	Infinity	-90.000	COORDBRK			-5.000	-29.000
4	Infinity	-29.000	SILICA	122.000	0.000	0.000	0.000
5	285.000	-685.000		122.000	0.000	0.000	0.000
6	850.000	0.000		636.013	0.000	0.000	0.000

CLAIMS

What is claimed is:

1. An apparatus for generating electricity from solar radiation comprising:

a dish reflector having a focus;

a fly's eye receiver held near said focus, including:

a field lens that concentrates sunlight into an image of said dish reflector;

a two-dimensional fly's eye array of contiguous convex lenses extending across said image;

a photovoltaic cell behind each convex lens of the fly's eye array, configured to receive light further concentrated by said convex lens; and

a structure configured to support and cool said photovoltaic cells; and

a dual axis tracking structure configured to hold said dish reflector and said fly's eye receiver in co-alignment and oriented to the sun;

wherein the photovoltaic cells are configured to convert said sunlight into electricity after being concentrated and divided between said photovoltaic cells in two imaging stages: in the first stage, said dish reflector and said field lens are together operative to concentrate the sunlight entering the apparatus in the form of the image of said dish, stabilized against pointing errors of said dual axis tracking structure, and in the second stage, said fly's eye array of contiguous convex lenses is operative to divide the sunlight energy of said image into portions, one per convex lens, each portion being further concentrated by said convex lens onto the photovoltaic cell behind said convex lens.

2. The apparatus for generating electricity from solar radiation of claim 1, wherein said dish reflector has the shape of a concave paraboloid with off-axis focus located to one side of the entering sunlight, so that said fly's eye receiver does not significantly block incoming sunlight.

3. The apparatus for generating electricity from solar radiation of claim 1, wherein the contiguous convex lenses in said fly's eye receiver are individually sized with the areas needed so that the portions of sunlight power from said image transmitted and further concentrated are equal.

4. The apparatus for generating electricity from solar radiation of claim 3, wherein the convex lenses in said fly's eye array each have focal length in proportion to their width, such that they all form images of the sun of close to the same diameter, and the linear displacements of said images are all the same for given mispointing angle.

5. The apparatus for generating electricity from solar radiation of claim 1, wherein said array of contiguous lenses has overall a concave, approximately spherical shape to better coincide with said pupil image, the center of said sphere being near said field lens, and the radius of said sphere being such that when the apparatus is correctly oriented to the sun, the light strikes each of the lenses in the array at close to normal angle of incidence, i.e. parallel to the lens axis.

6. The apparatus for generating electricity from solar radiation of claim 1, further comprising a tertiary optical element in the form of a dome lens introduced just ahead of each cell, wherein said dome lens is operative to more evenly distribute the light focused by the fly's eye lens element onto the cell and to increase tolerance to mispointing.

7. The apparatus for generating electricity from solar radiation of claim 1, further comprising a tertiary optical element in the form of an optical funnel introduced just ahead of each cell, wherein said funnel is operative to more evenly distribute the light focused by the fly's eye lens element onto the cell and to increase tolerance to mispointing.

8. The apparatus for generating electricity from solar radiation of claim 1, wherein said fly's eye receiver is sealed against contamination, by said field lens at its entrance and by a continuous concave bowl supporting the multiplicity of cells at its rear.

9. The apparatus for generating electricity from solar radiation of claim 1, wherein said cells are supported by a thermally conductive bowl with a multiplicity of finned heatsinks behind, said heatsinks being cooled by forced air convection.

10. The apparatus for generating electricity from solar radiation of claim 1, wherein said cells are supported by a thermally conductive bowl cooled from behind by thermal transfer liquid pumped to a radiator or for use as a source of solar thermal power.

11. The apparatus for generating electricity from solar radiation of claim 1, wherein said field lens is made of fused silica coated by two or more successively deposited sol-gel layers of different density and thickness, operative to form a broad-band antireflection coating.

12. The apparatus for generating electricity from solar radiation of claim 1, wherein the lenses of the fly's eye array are made of glass which has been heat treated to cause phase separation, and chemically leached so as to reduce surface reflection over a broad spectral band.

13. The apparatus for generating electricity from solar radiation of claim 1, further comprising one or more dish/receiver units as described above, supported on a dual-axis tracking mount, said mount being adapted to position said unit or units toward the sun and to

track the movement of the sun across the sky so that solar radiation from the sun illuminates said dish-shaped reflectors and is reflected from said dish-shaped reflectors toward said field lenses associated with each said dish-shaped reflector.

14. A broadband antireflection coating for fused silica, comprising:

two successively deposited sol-gel layers of different refractive index, both indices being less than that of silica, and having a bottom layer with higher refractive index than a top layer, wherein the refractive index of the bottom layer is between 1.3 and 1.4, and the refractive index of the top layer is between 1.1 and 1.3, each layer having a thickness between 100 nm and 130 nm.

15. The broadband antireflection coating for fused silica according to claim 14, wherein each layer is deposited via a spin coating technique.

16. A method for broadband antireflection coating of a hot-pressed high-borate (10-20% borate) borosilicate glass lens, comprising the steps of:

preparing a lens by phase separation, by heat-treating at 570-650°C for 6-24 hours, then removing the molding contamination by soaking in 5-15% ammonium bifluoride; and

leaching the lens in a mineral acid at 20-25%, with 1.5% ammonium bifluoride added for 5-20 minutes at 40-80°C.

17. A method for forming as a single piece a glass lens array with a multiplicity of contiguous individual convex lenses on one side and a smooth curve or flat on the other, comprising the steps of:

preparing a mold having a first face with a multiplicity of sharp boundaries to form a first, quilted surface of the contiguous lenses of a lens array, and a second smoothly curved face;

heating a glass preform the size of the array to softening;

hot pressing said glass preform in said mold, with said second face lowermost, until imprinting said glass with the quilted surface is complete;

removing said first face of the mold before cooling, the glass resting on said second, smoothly curved mold face; and

rapidly cooling the glass and second mold face to freeze in the shape;

wherein said lens array so formed has sharp boundaries of the quilted surface preserved, with minimal blurring effects from differential expansion between said glass and said mold face.

18. The method of claim 17, wherein, during cooling, the glass is heat-treated to cause phase separation while being supported from its second surface to avoid thermal deformation.

19. A method for forming a lens array from individual press-molded lenses, comprising the steps of:

mounting a plurality of lenses individually on concentric hubs in an array;

cutting said hub-mounted lenses accurately into the individual, differently-shaped segments of the array as needed to fit together with minimal gaps between;

mounting said hubs with cut lenses still attached into an assembly jig, made so said hubs hold in position said lenses as required to accurately form the array;

bonding said lenses to each other to form a single rigid fly's eye array; and

removing said array from the hubs and jig;

wherein said lens array so formed is operative to concentrate entering light into multiple foci with minimal geometric losses because the boundaries have been sharply defined.

20. The method for forming a lens array from individual press-molded lenses according to claim 19, wherein the bonding step comprises bonding by wicked-in adhesive.

21. A method for forming a fly's eye lens array, comprising the steps of:

cutting individual press-molded lenses into individual, differently-shaped lens segments needed to form a fly's eye lens array with minimal gaps, the cut sides of said segments being provided with small locating notches cut into the middles of the sides, away from the convex aspheric sides of the lenses; and

bonding said lens segments to a supporting structure made with square openings, each sized to match a lens segment, and with small tabs to engage with lens-locating notches to ensure correct lateral positioning of the lenses in the fly's eye lens array;

wherein said lens array with said supporting structure attached is operative to concentrate entering light into multiple foci, with minimal geometric losses because the lens boundaries have been sharply defined, and because said square openings of said supporting structure are large enough to avoid blocking the light refracted by said lens segments toward multiple foci.

22. A dual axis, altitude-azimuth tracker to carry solar reflectors comprising:

a rigid triangular azimuth spaceframe structure with wheels at each of three lower corner nodes riding on a circular ground track to support the tracker weight and drive it in

rotation, and with a lower central node attached to a ground anchor so as to constrain lateral decentering motion and prevent wind lift;

a rigid elevation structure hinged at two upper nodes of said azimuth structure and driven in elevation by a linear actuator from a third node of said azimuth structure;

solar reflectors carried by said elevation structure;

and wherein accurate orientation of the reflectors with respect to the sun is maintained independent of irregularities or levelling of said track, by driving said elevation actuator and one or more of said wheels, based on information from encoders and from some combination of solar and level sensors carried by said elevation structure, and calibration data.

23. The apparatus for generating electricity from solar radiation of claim 1, carried by the dual axis tracker of claim 22 further comprising arms attached to said elevation structure and projecting out from under said reflectors to support said fly's eye receivers.

24. The dual axis tracker of claim 22, wherein said azimuth spaceframe structure comprises preformed subassemblies with preformed nodes and mechanical elements such as wheels, bearings and actuators, and premanufactured lightweight struts, and wherein assembly in the field is accomplished largely by connecting said nodes and said subassemblies.

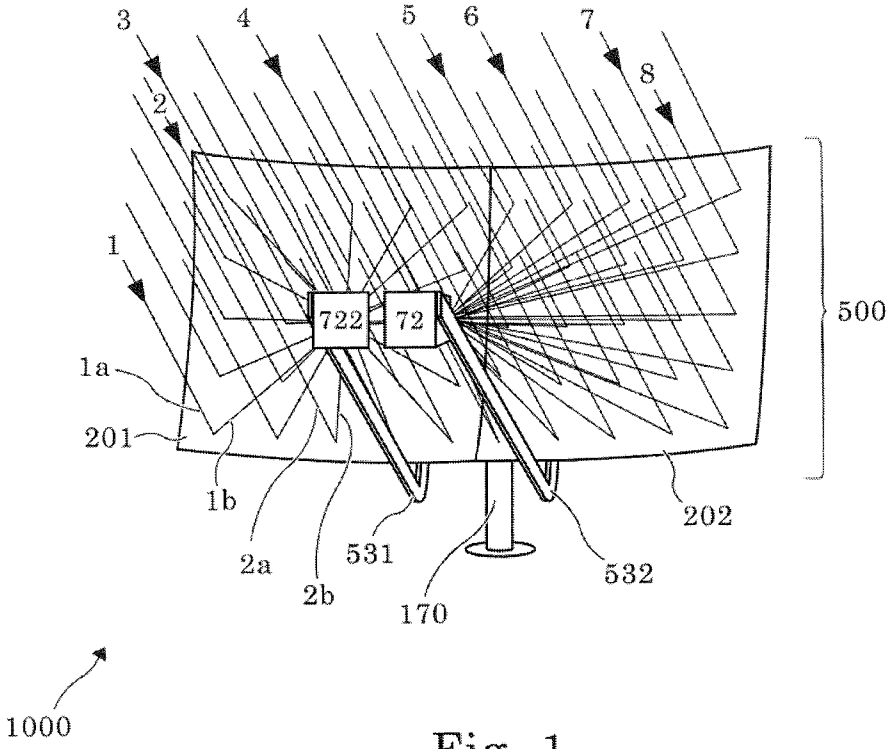


Fig. 1

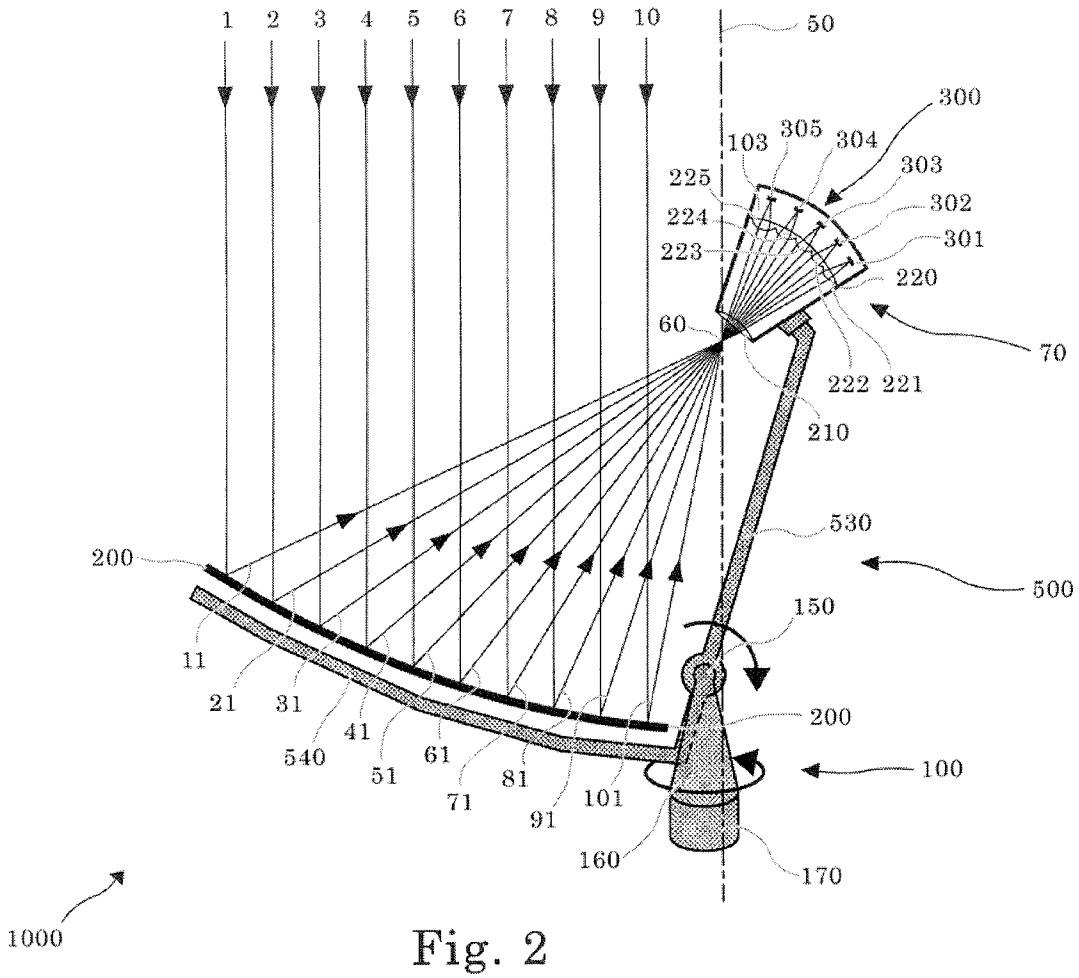

1
2
3
4
5
6
7
8
9
10
50
300
103
305
304
303
225
302
224
301
223
220
60
70
222
221
210
530
200
500
150
11
21
31
41
540
51
61
71
81
91
101
200
100
160
170
1000

Fig. 2

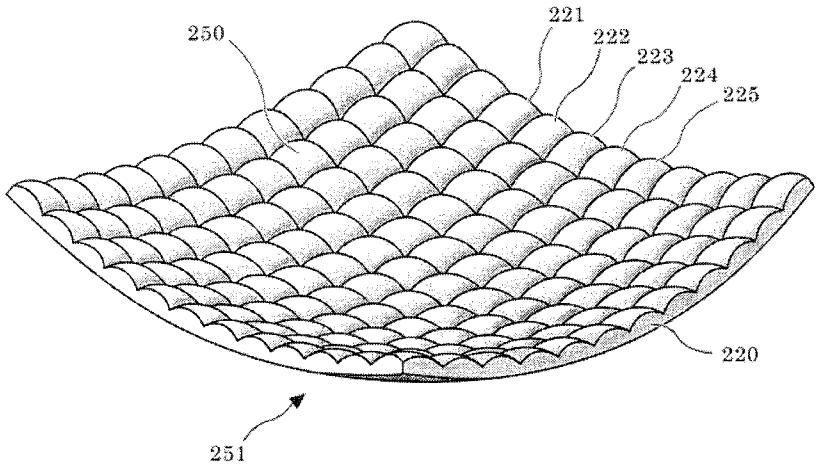


Fig. 3

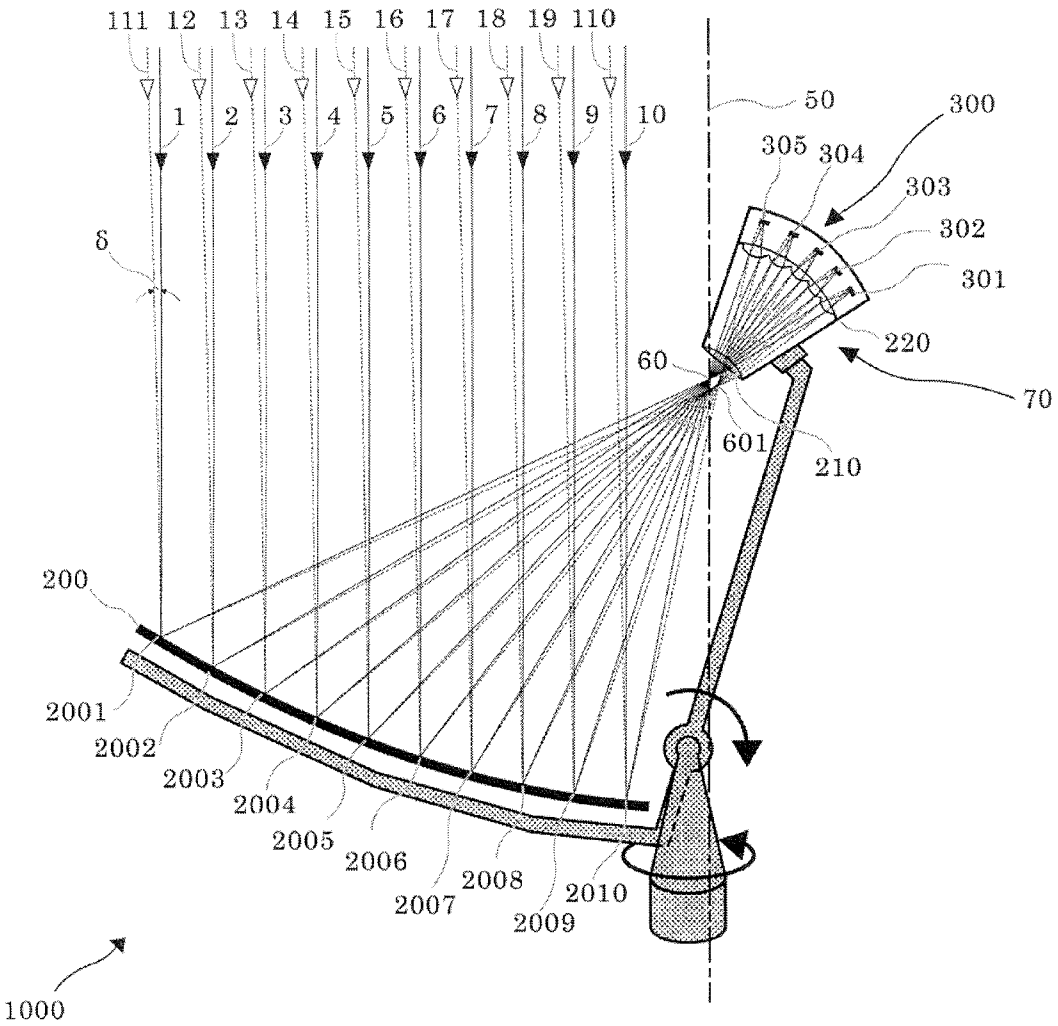

111 12 13 14 15 16 17 18 19 110
1 2 3 4 5 6 7 8 9 10
δ
50
300
305 304
303
302
301
220
70
60
601
210
200
2001
2002
2003
2004
2005
2006
2007
2008
2009
2010
1000

Fig. 4

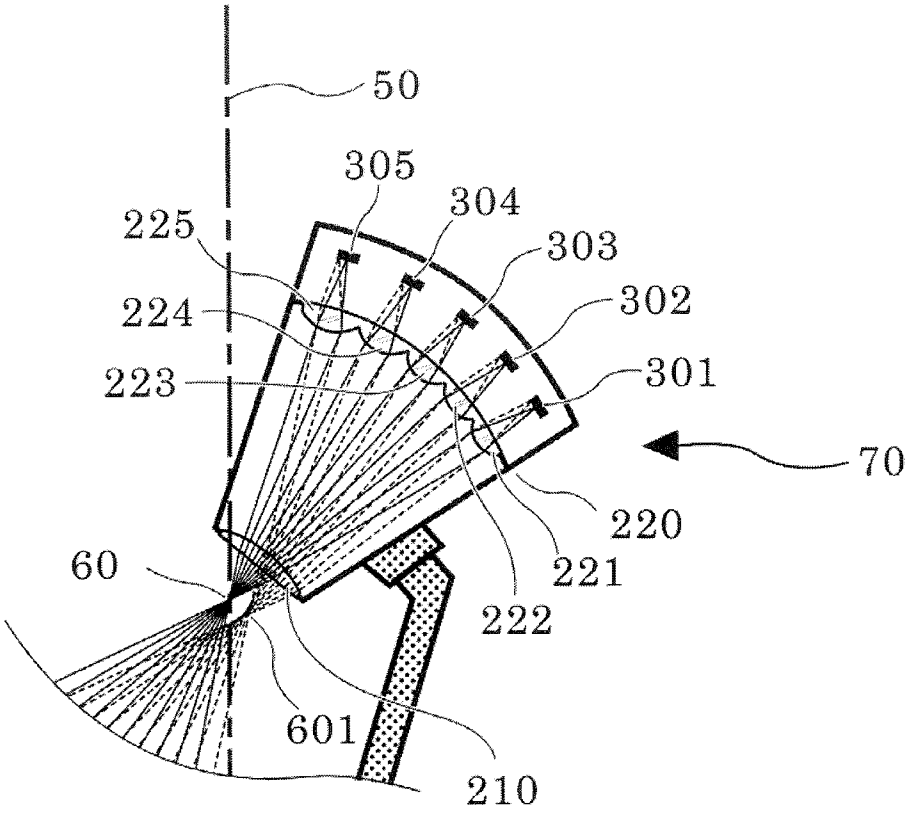


Fig. 5

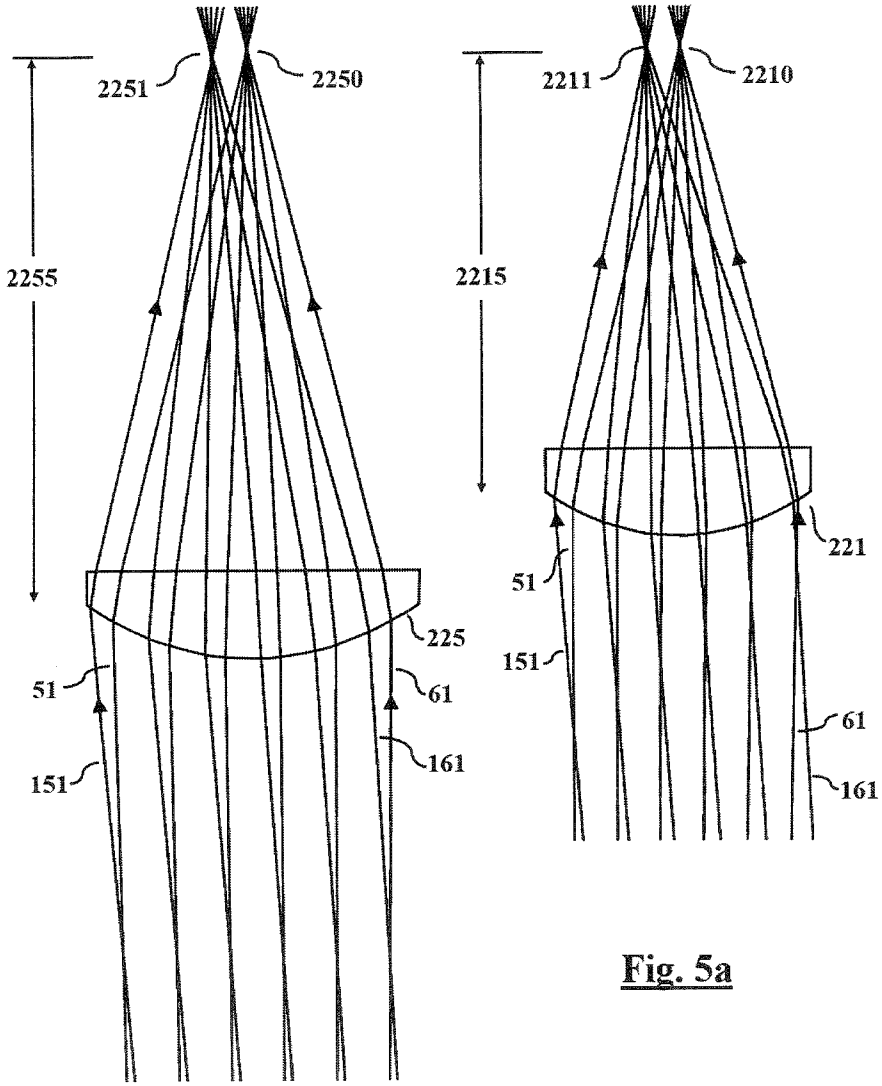

2251
2250
2255
225
51
61
151
161
2211
2210
2215
221
51
151
61
161

Fig. 5a

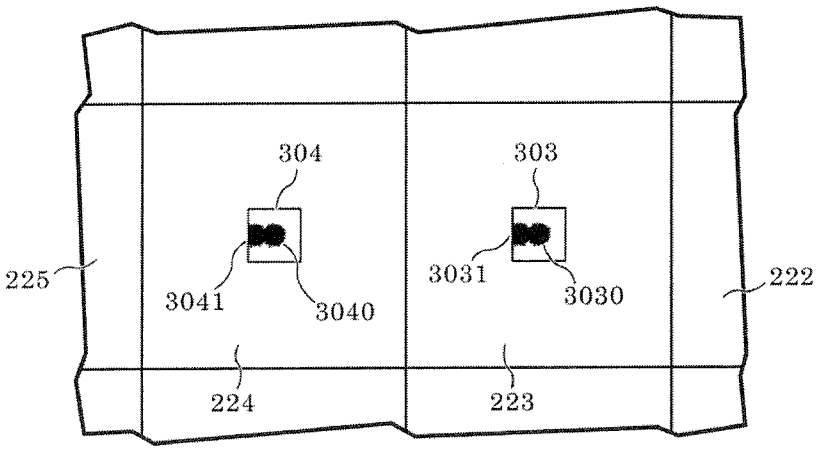


Fig. 6

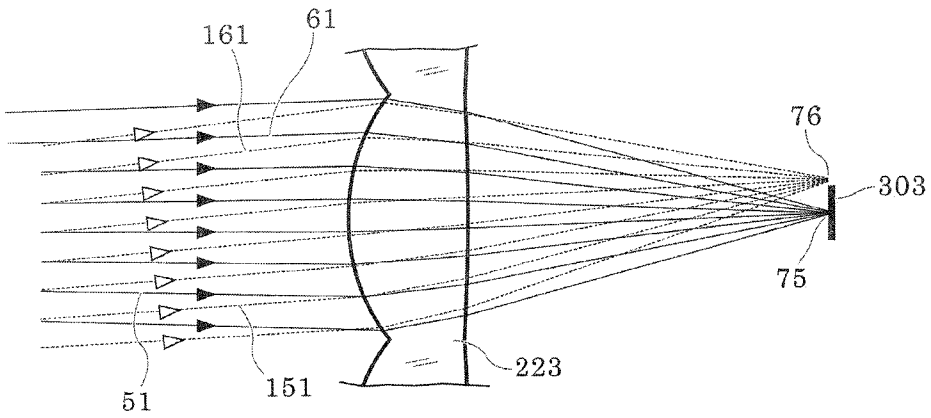


Fig. 7a

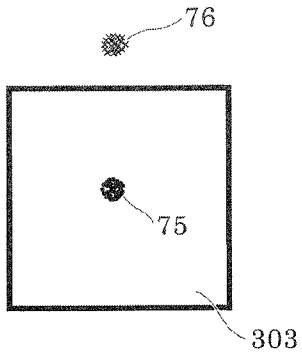


Fig. 7c

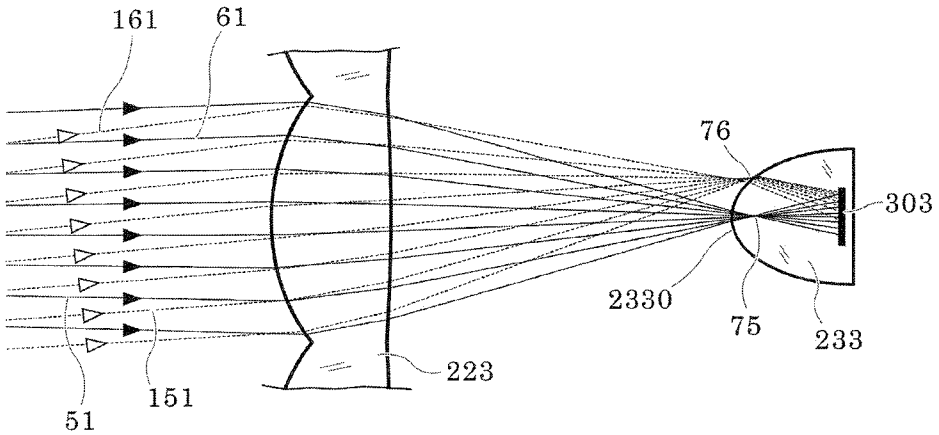


Fig. 7b

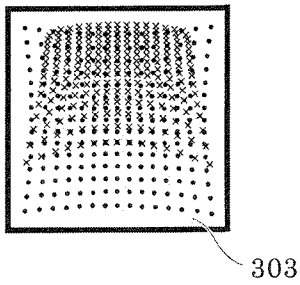


Fig. 7d

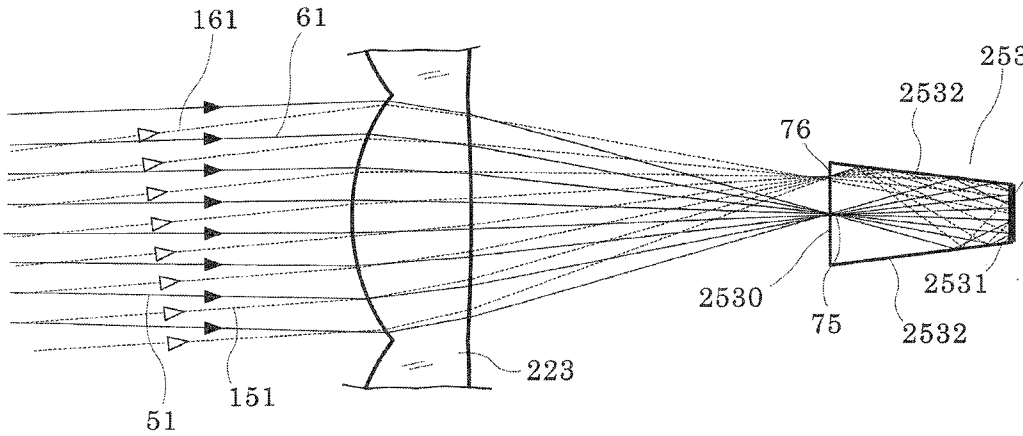


Fig. 7e

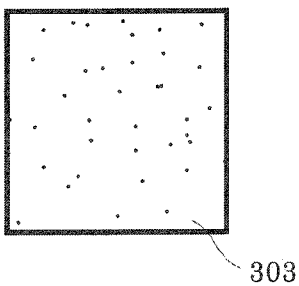


Fig. 7f

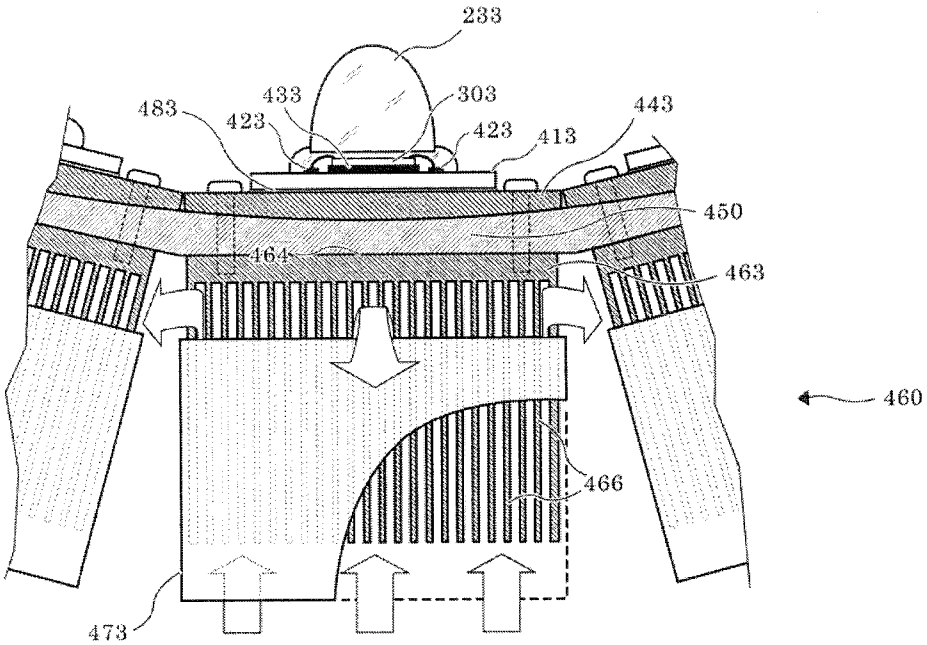

233
433
303
483
423
423
413
443
450
464
463
460
466
473

Fig. 8a

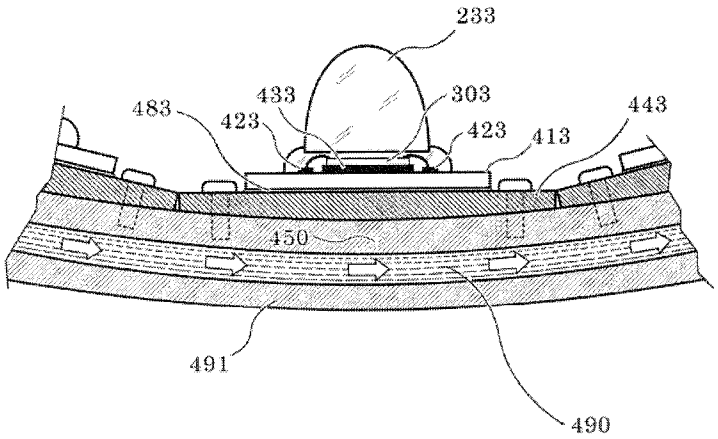

233
433
303
483
423
423
413
443
450
491
490

Fig. 8b

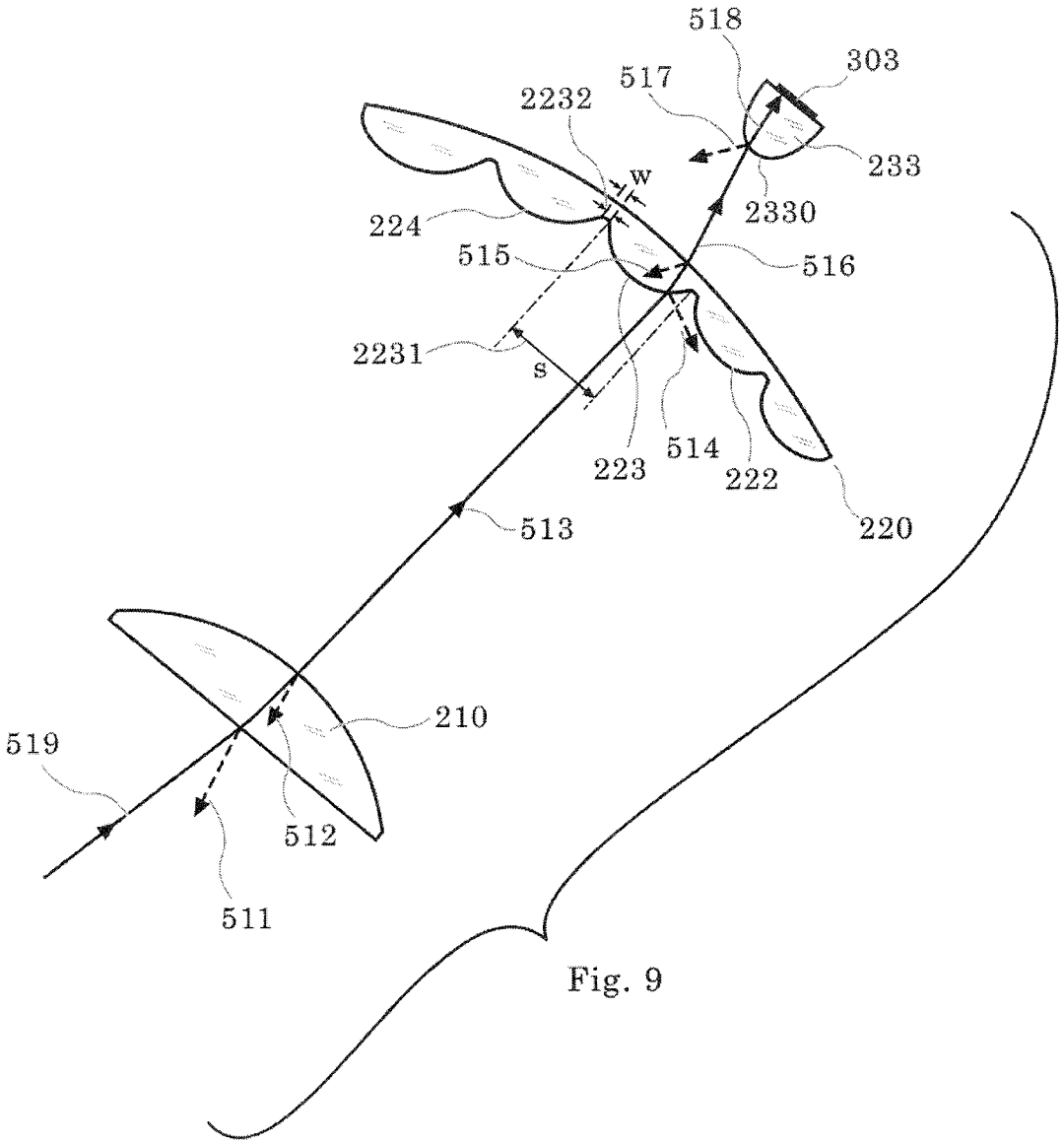

518
303
517
2232
233
w
2330
224
515
516
2231
s
223
514
222
220
513
210
519
512
511

Fig. 9

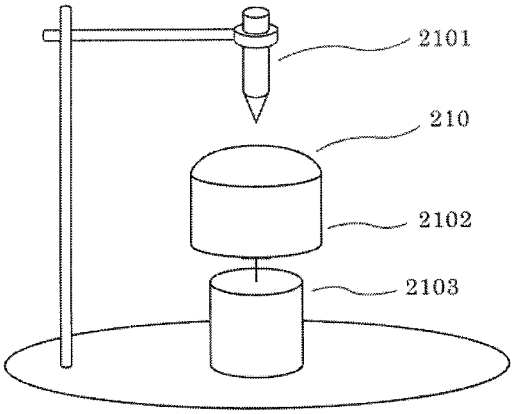


Fig. 10a

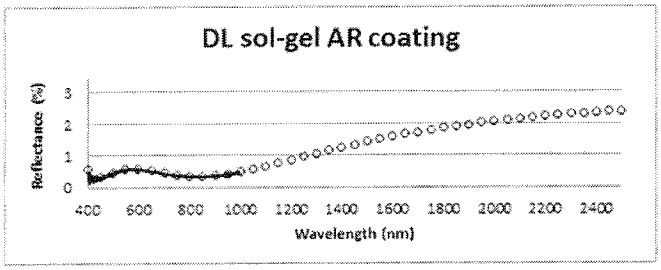


Fig. 10b

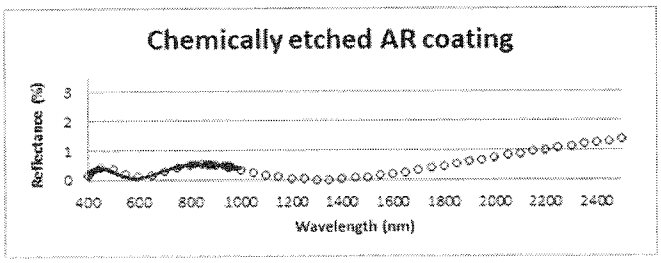


Fig. 11

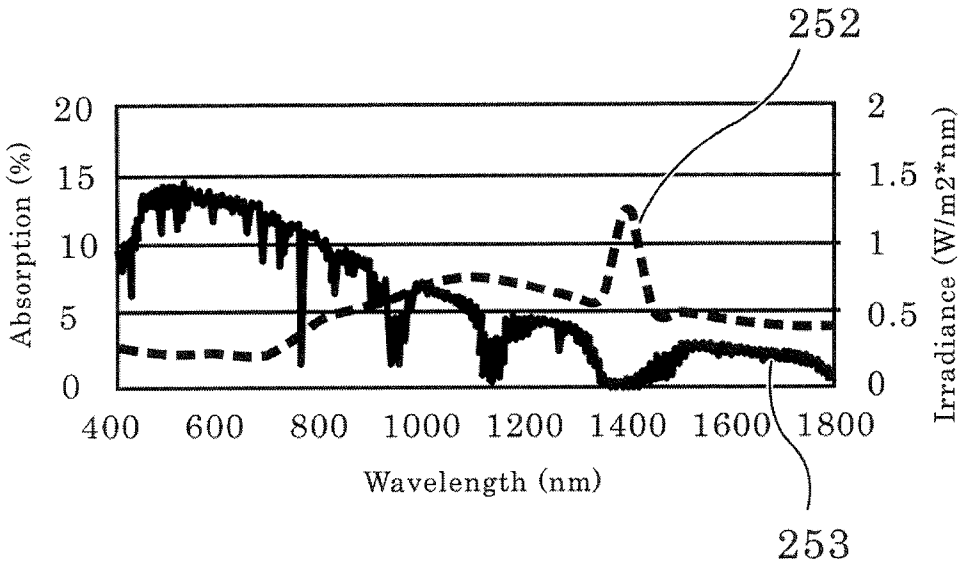

252
20
15
10
5
0
Absorption (%)
2
1.5
1
0.5
0
Irradiance (W/m2*nm)
400
600
800
1000
1200
1400
1600
1800
Wavelength (nm)
253

Fig. 12

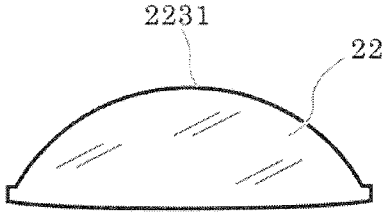


Fig. 13a

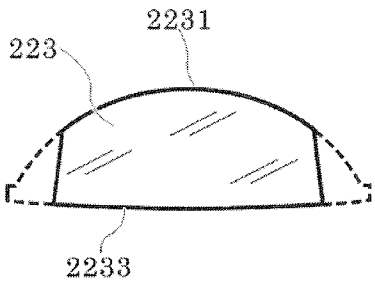


Fig. 13b

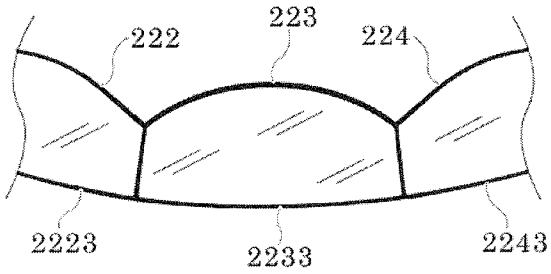


Fig. 13c

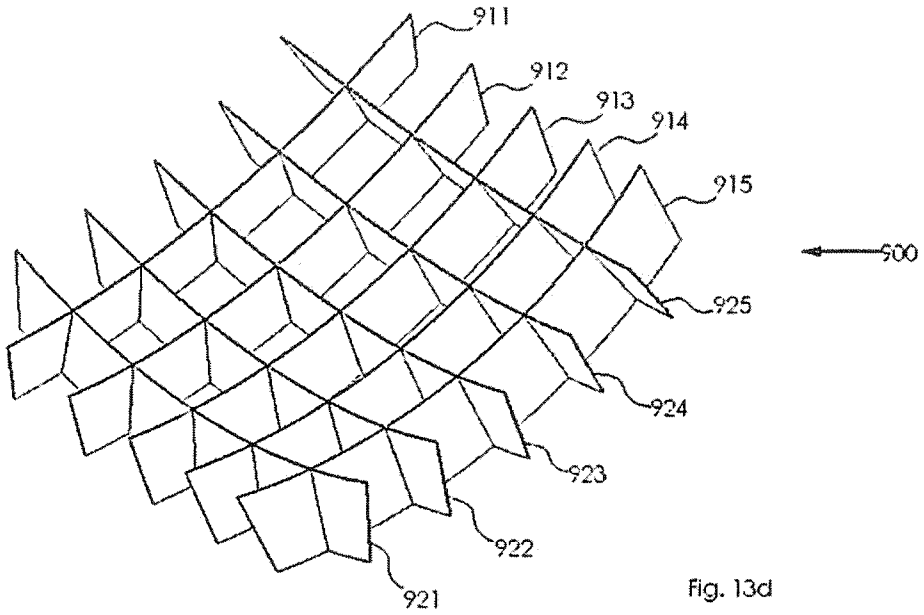


Fig. 13d

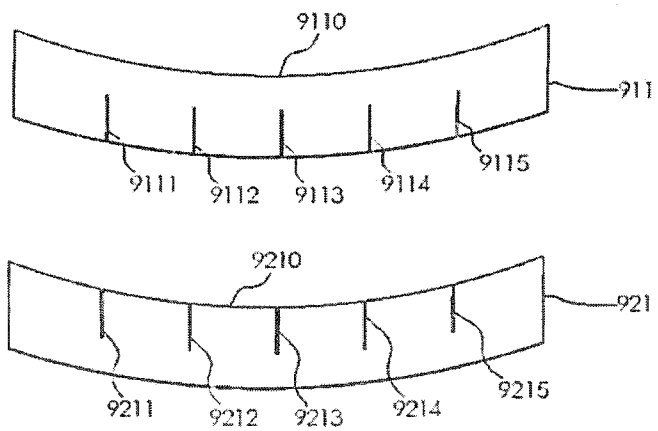


Fig. 13e

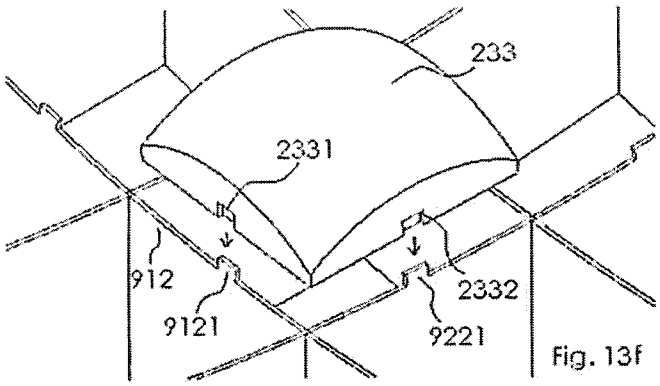


Fig. 13f

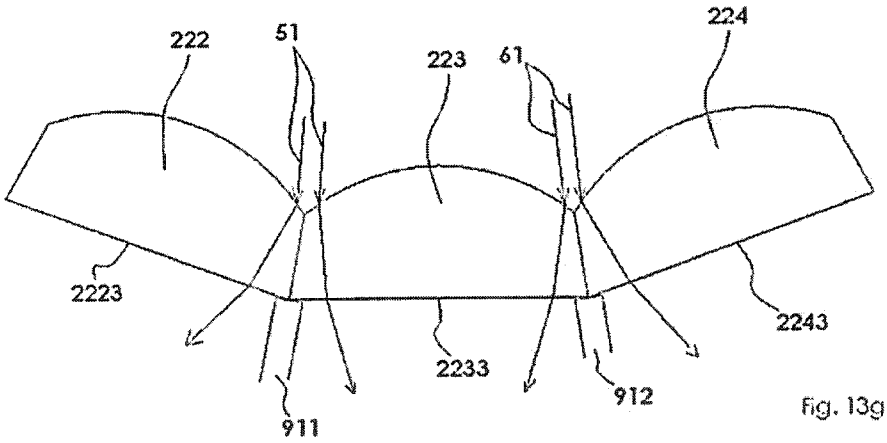


Fig. 13g

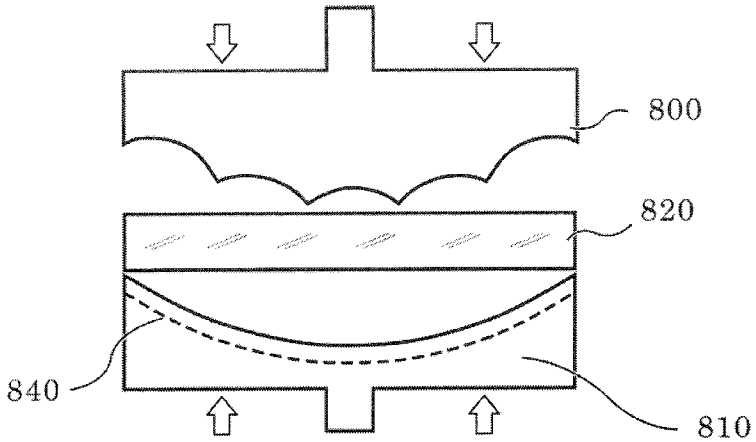


Fig. 14a

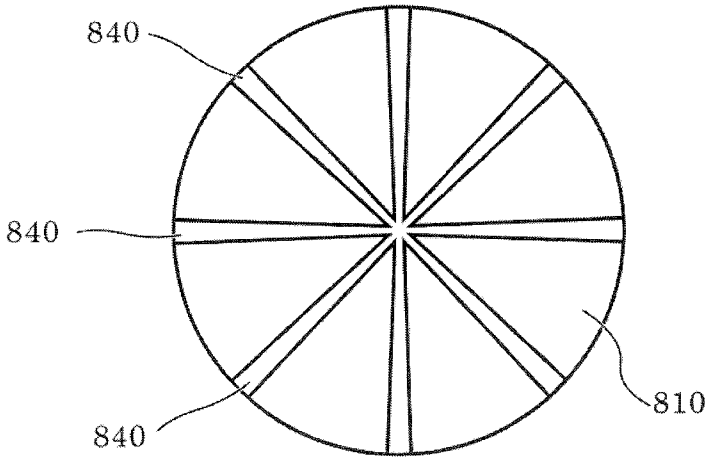


Fig. 14b

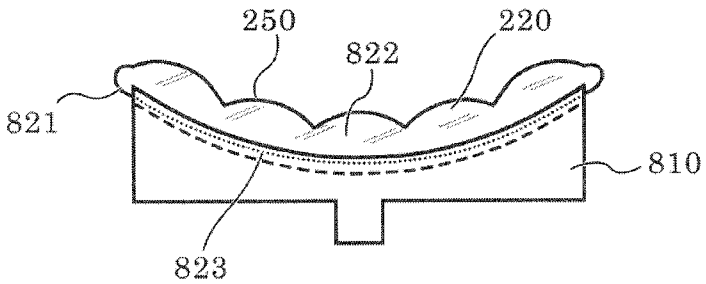


Fig. 14c

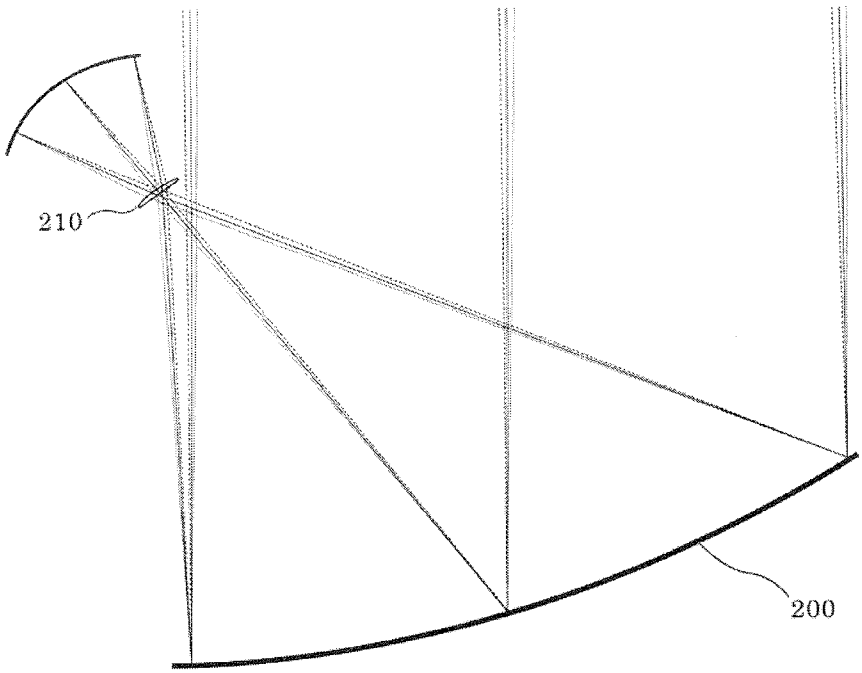


Fig. 15a

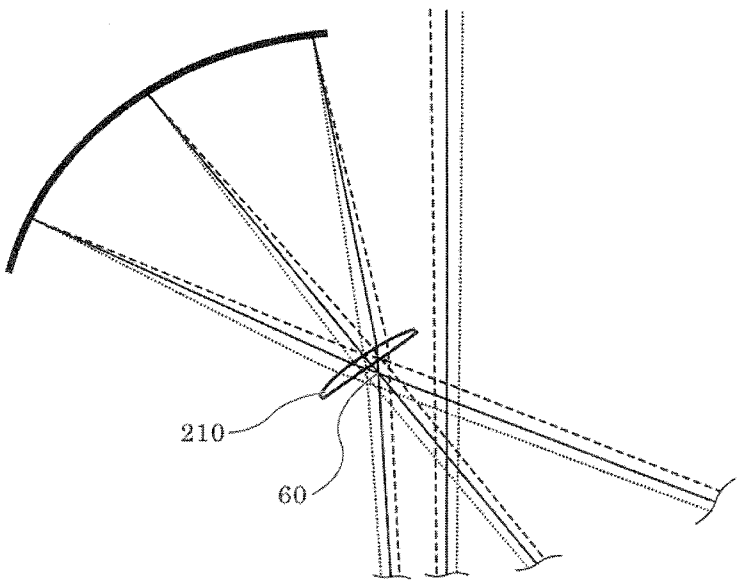


Fig. 15b

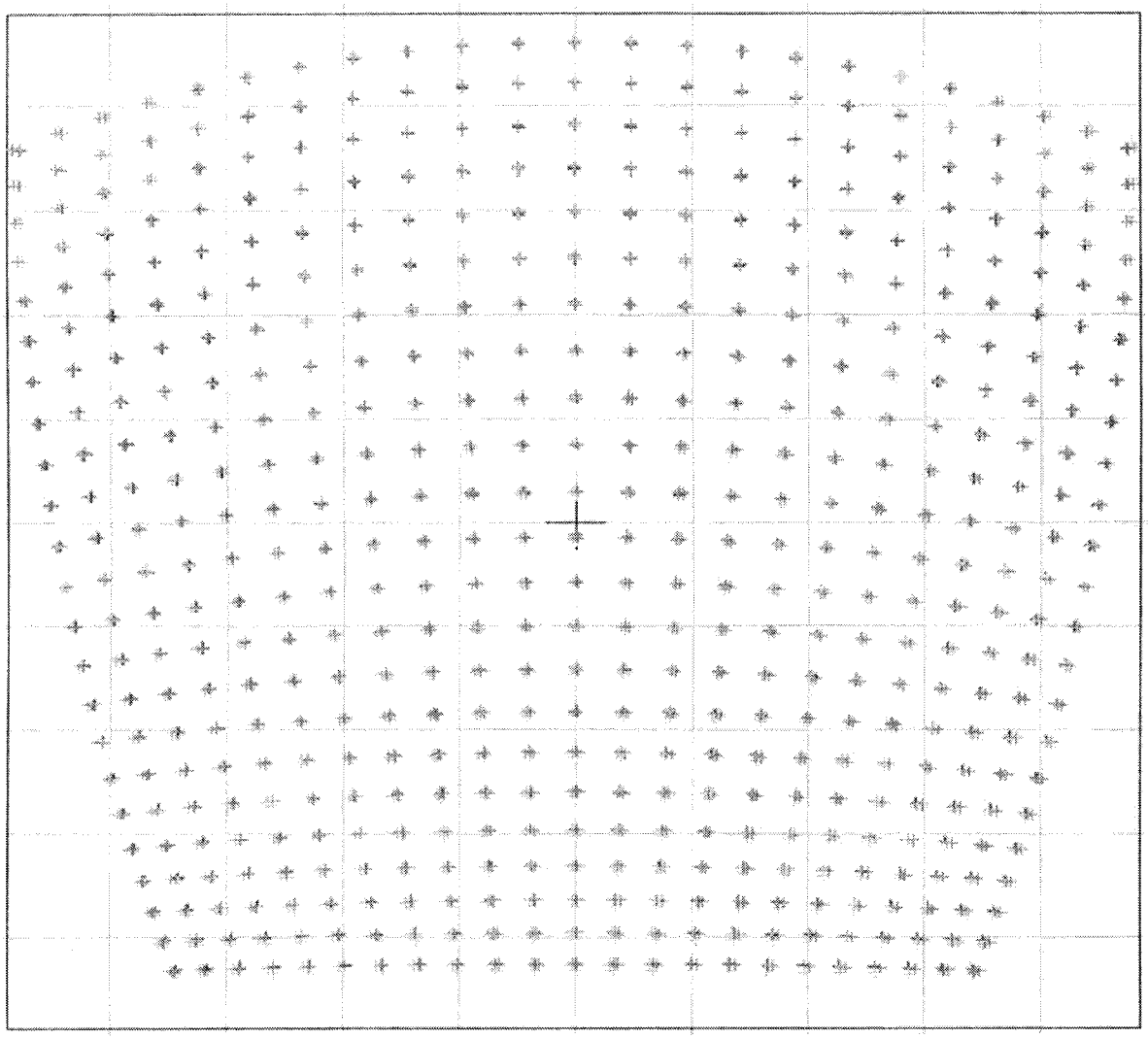


Fig. 16

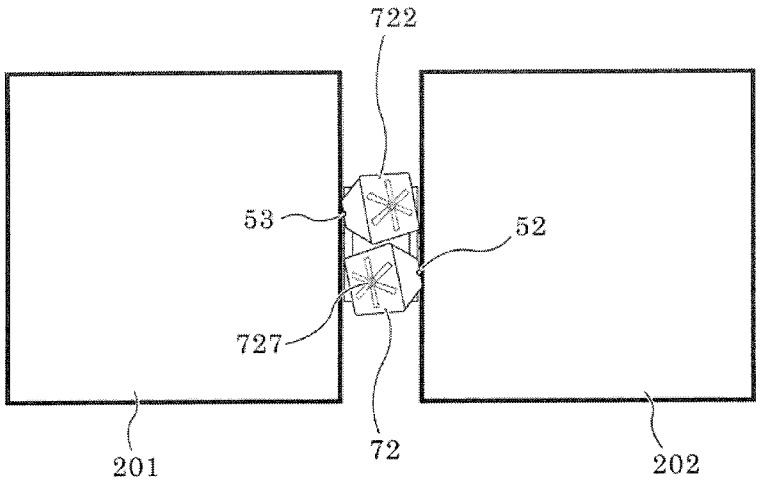


Fig. 17a

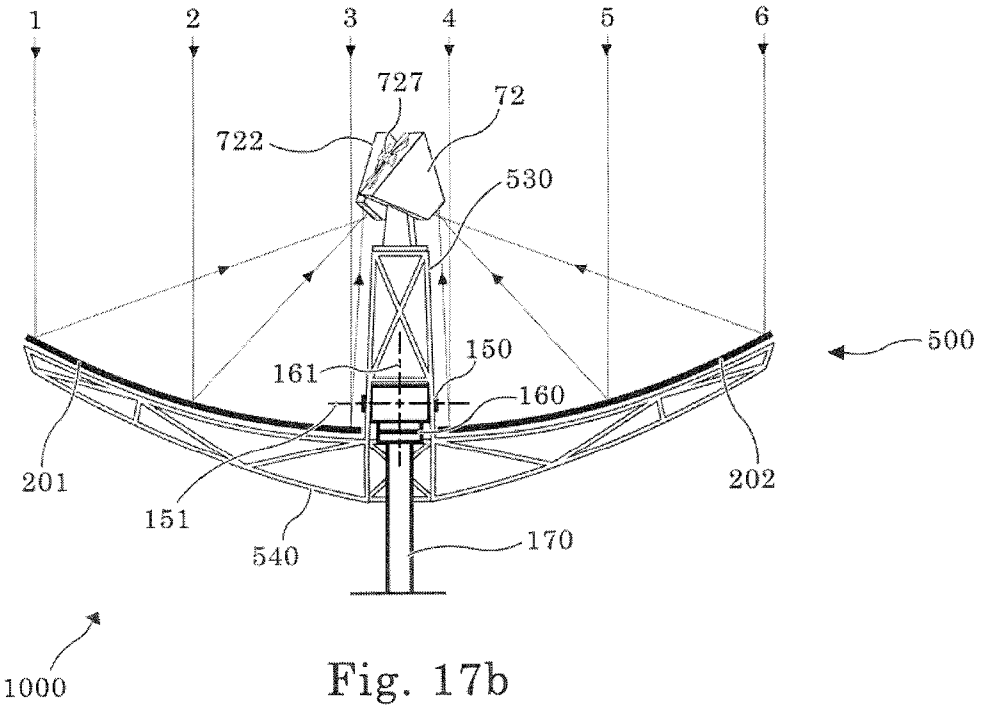


Fig. 17b

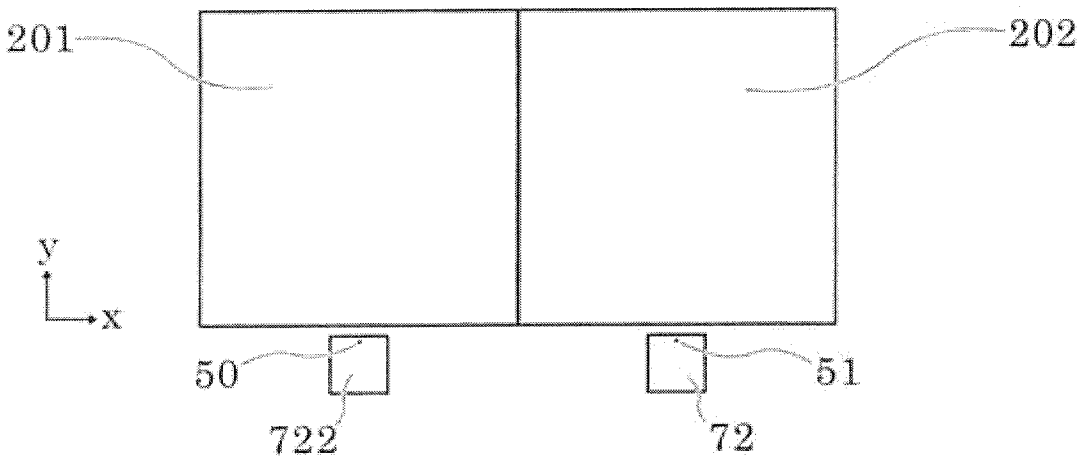


Fig. 18

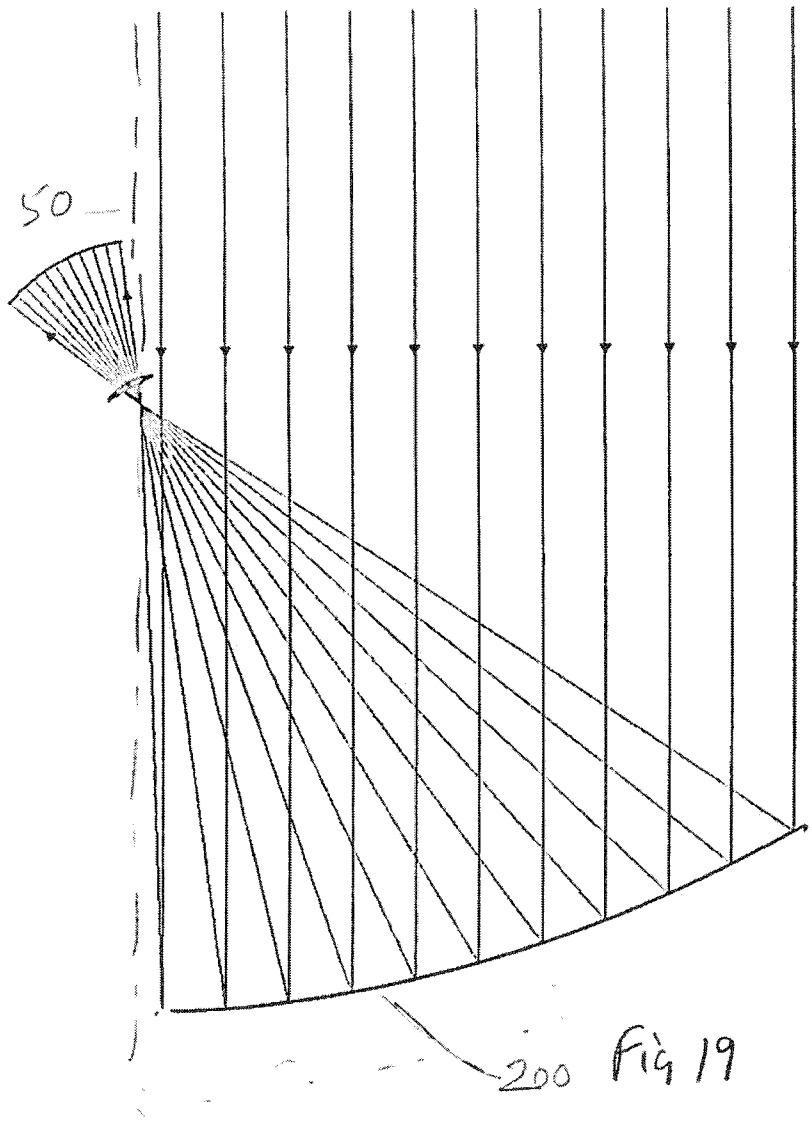


Fig 19

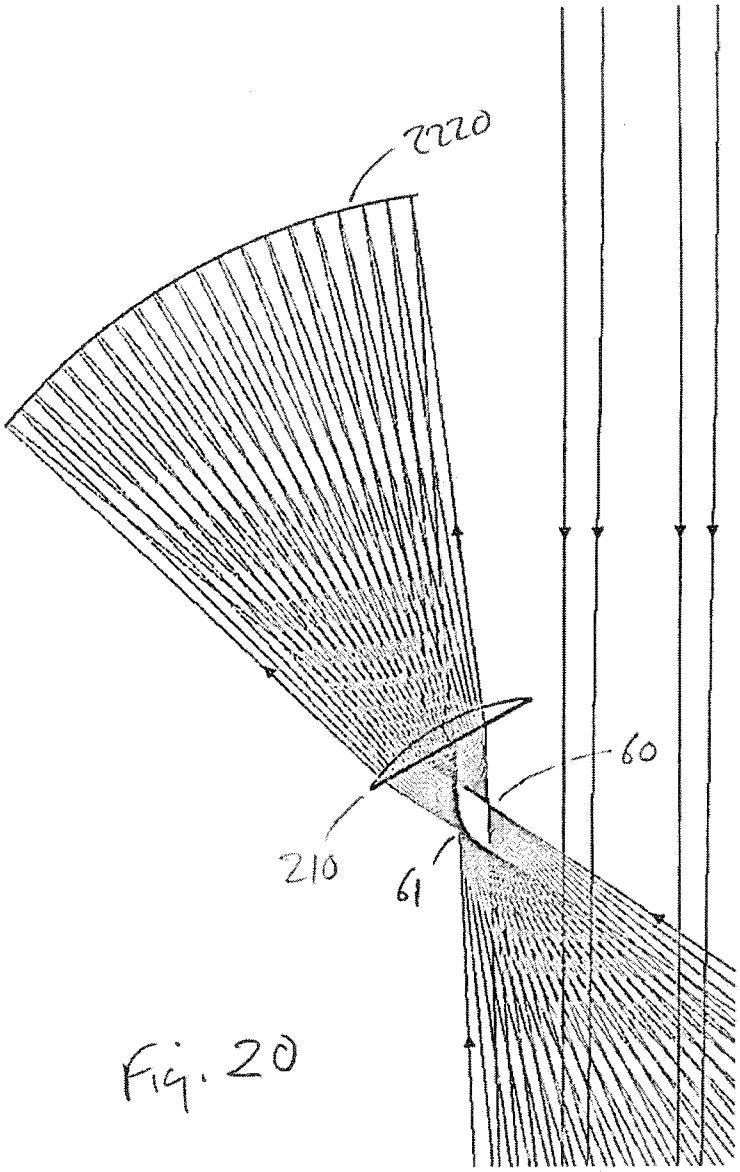


Fig. 20

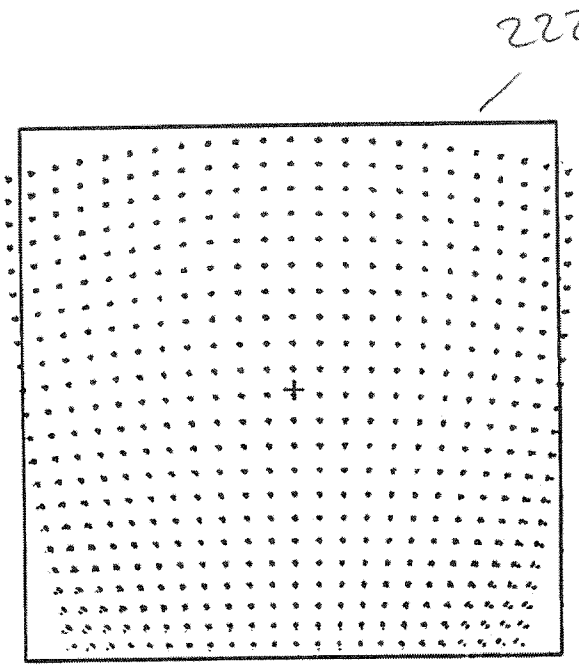


Fig. 21

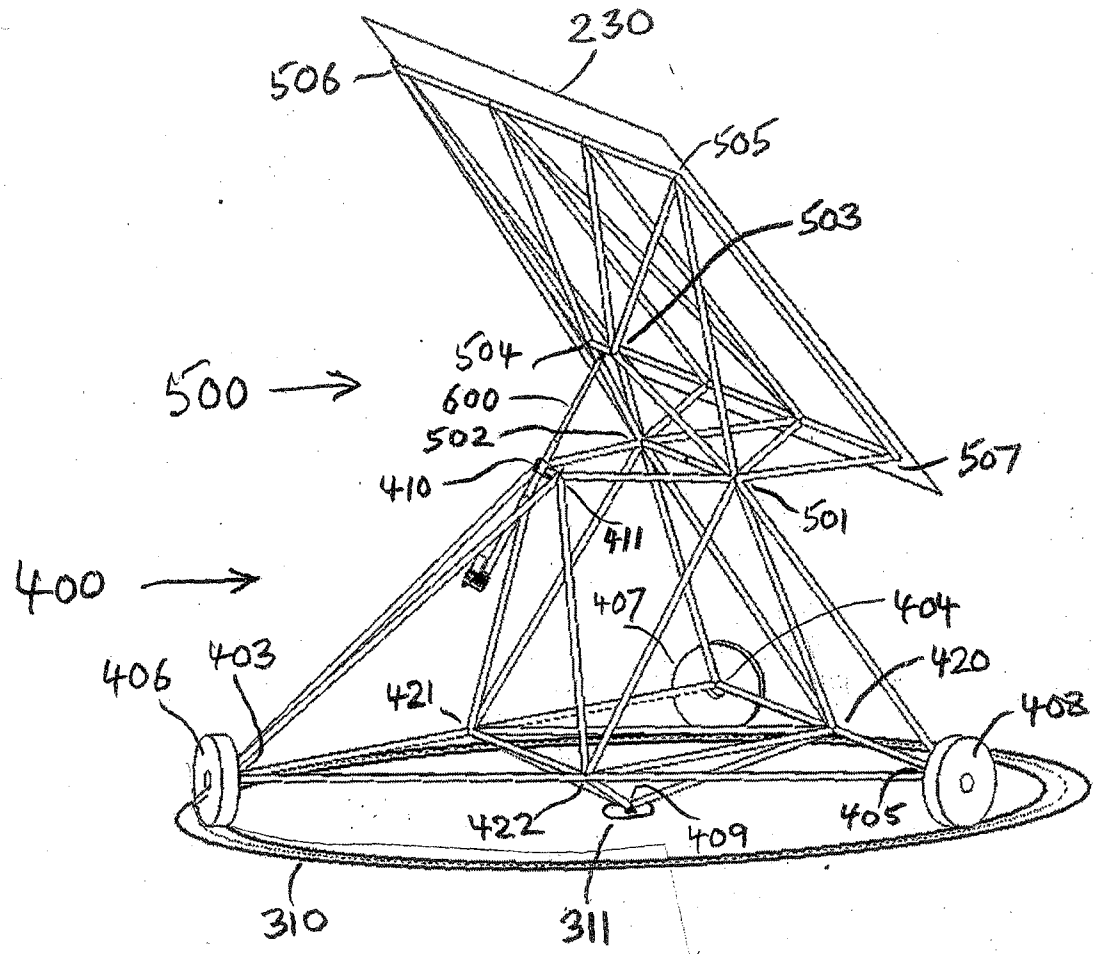

230
506
505
503
504
500
600
502
507
410
501
411
400
407
404
406
403
420
421
408
422
409
405
310
311

Fig. 22

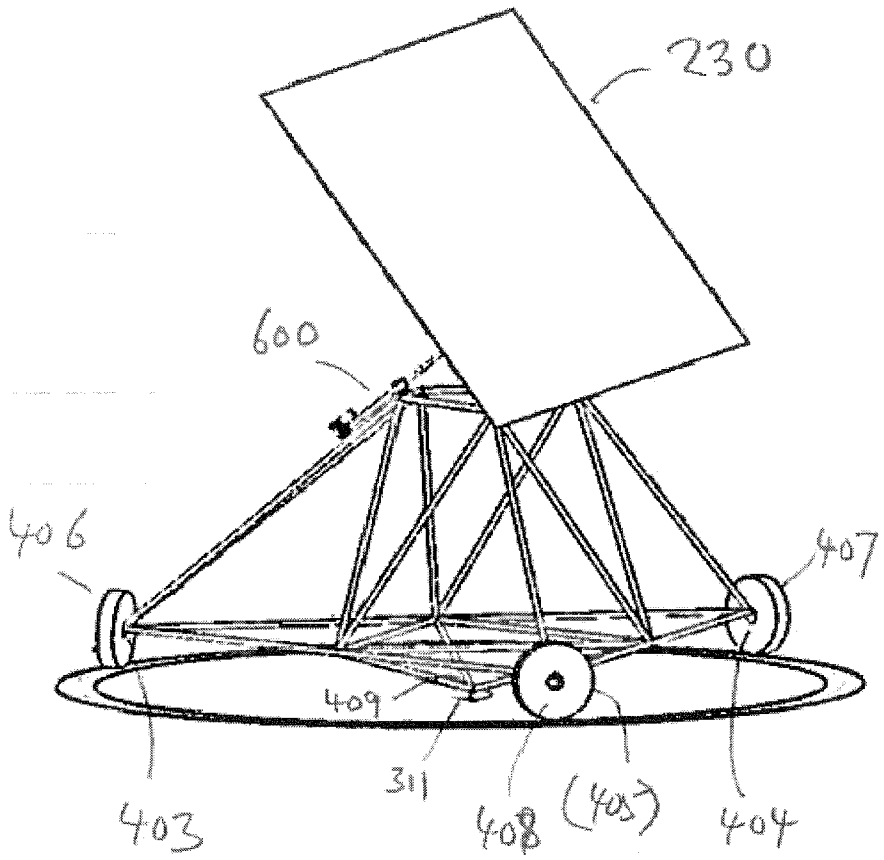


Fig 23

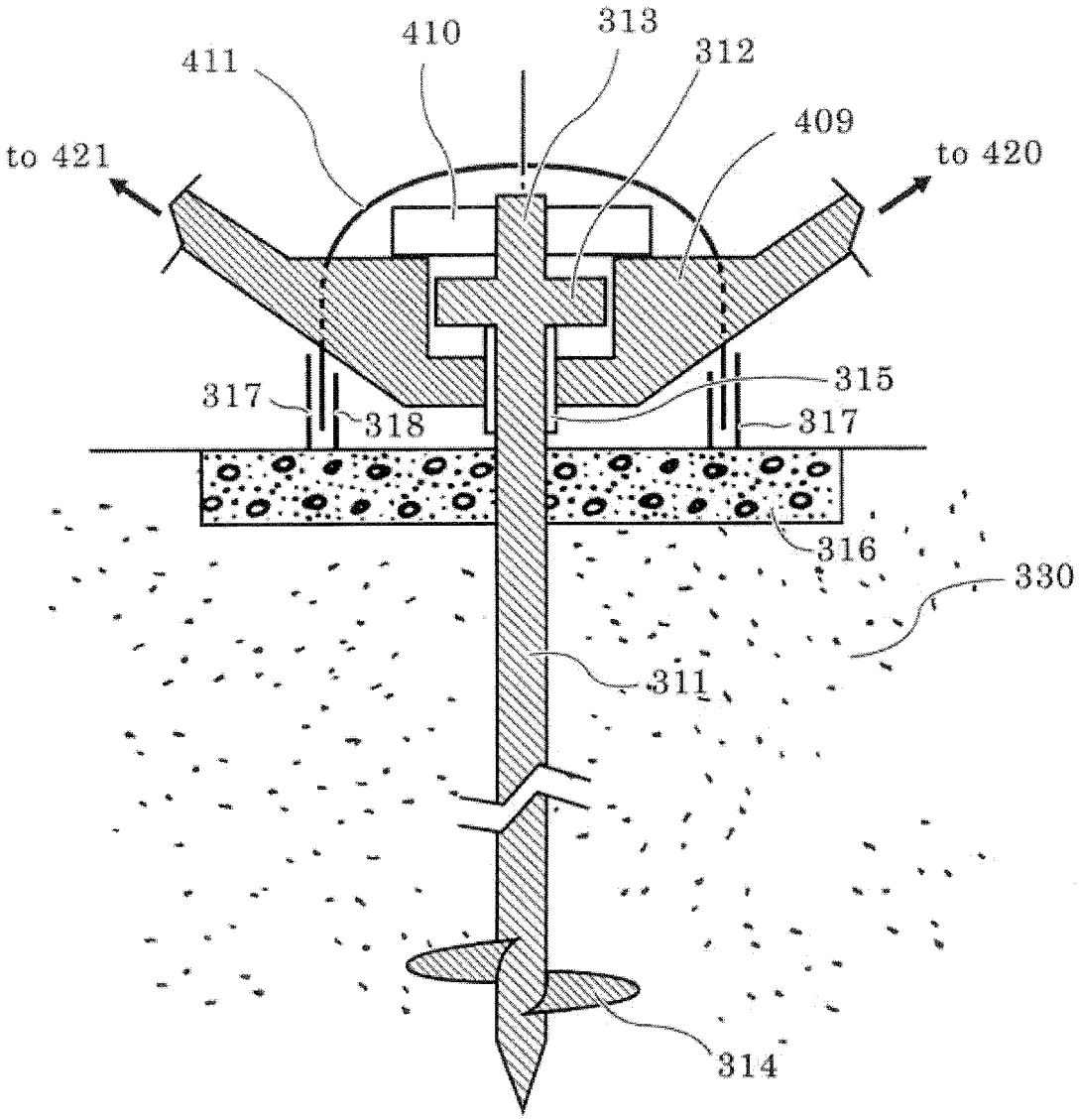


Fig. 24

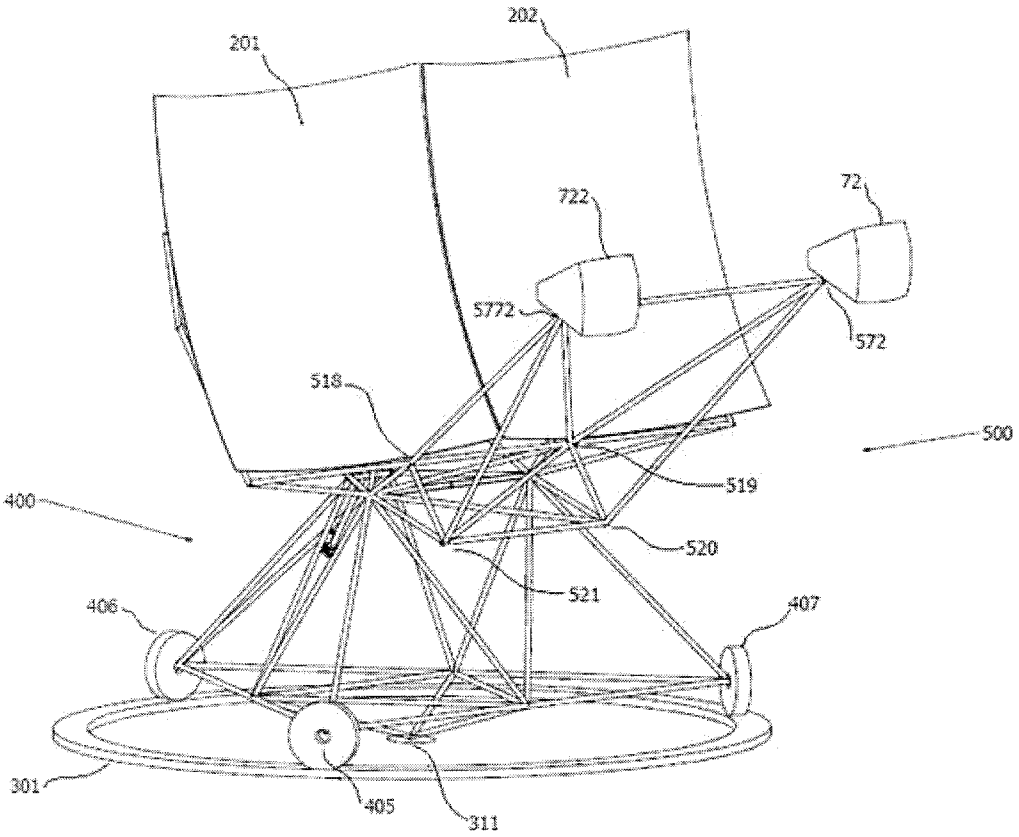

202
201
722
72
5772
572
518
500
519
400
520
521
406
407
301
405
311

FIG. 25

INTERNATIONAL SEARCH REPORT

International application No.
PCT/US 18/30491

A. CLASSIFICATION OF SUBJECT MATTER
IPC(8) - F24J 2/08; H01L 31/054; H02S 20/32; H02S 40/22 (2018.01)
CPC - F24S 23/70; F24S 30/45; H01L 31/0543; H01L 31/0547; H02S 20/32; H02S 40/22; Y02E 10/47; Y02E 10/52

According to International Patent Classification (IPC) or to both national classification and IPC

B. FIELDS SEARCHED

Minimum documentation searched (classification system followed by classification symbols)
See Search History Document

Documentation searched other than minimum documentation to the extent that such documents are included in the fields searched
See Search History Document

Electronic data base consulted during the international search (name of data base and, where practicable, search terms used)
See Search History Document

C. DOCUMENTS CONSIDERED TO BE RELEVANT

Category*	Citation of document, with indication, where appropriate, of the relevant passages	Relevant to claim No.
A	US 2015/0303867 A1 (ARIZONA BOARD OF REGENTS ON BEHALF OF UNIVERSITY OF ARIZONA) 22 October 2015 (22.10.2015), Fig 1, 2a, 2b, 36, abstract, para [0091]-[0093], [0174]	1-13
A	US 2008/0185034 A1 (CORIO) 07 August 2008 (07.08.2008), Fig 4, abstract, para [0045], [0046]	1-13
A	US 2012/0192919 A1 (MIZUYAMA) 02 August 2012 (02.08.2012), Fig 2, abstract, para [0032]	1-13
A	US 2013/0068285 A1 (NI et al.) 21 March 2013 (21.03.2013), Fig 1, abstract, para [0019]	1-13
A	US 2014/0261392 A1 (LAMBRECHT) 18 September 2014 (18.09.2014), Fig 6A, abstract, para [0031], [0039], [0043]	1-13

☐ Further documents are listed in the continuation of Box C. ☐ See patent family annex.

* Special categories of cited documents:
"A" document defining the general state of the art which is not considered to be of particular relevance
"E" earlier application or patent but published on or after the international filing date
"L" document which may throw doubts on priority claim(s) or which is cited to establish the publication date of another citation or other special reason (as specified)
"O" document referring to an oral disclosure, use, exhibition or other means
"P" document published prior to the international filing date but later than the priority date claimed
"T" later document published after the international filing date or priority date and not in conflict with the application but cited to understand the principle or theory underlying the invention
"X" document of particular relevance; the claimed invention cannot be considered novel or cannot be considered to involve an inventive step when the document is taken alone
"Y" document of particular relevance; the claimed invention cannot be considered to involve an inventive step when the document is combined with one or more other such documents, such combination being obvious to a person skilled in the art
"&" document member of the same patent family

Date of the actual completion of the international search	Date of mailing of the international search report
30 August 2018	18 SEP 2018

Name and mailing address of the ISA/US	Authorized officer:
Mail Stop PCT, Attn: ISA/US, Commissioner for Patents P.O. Box 1450, Alexandria, Virginia 22313-1450 Facsimile No. 571-273-8300	Lee W. Young PCT Helpdesk: 571-272-4300 PCT OSP: 571-272-7774

INTERNATIONAL SEARCH REPORT

International application No.
PCT/US 18/30491

Box No. II Observations where certain claims were found unsearchable (Continuation of item 2 of first sheet)

This international search report has not been established in respect of certain claims under Article 17(2)(a) for the following reasons:

1. ☐ Claims Nos.:
because they relate to subject matter not required to be searched by this Authority, namely:

2. ☐ Claims Nos.:
because they relate to parts of the international application that do not comply with the prescribed requirements to such an extent that no meaningful international search can be carried out, specifically:

3. ☐ Claims Nos.:
because they are dependent claims and are not drafted in accordance with the second and third sentences of Rule 6.4(a).

Box No. III Observations where unity of invention is lacking (Continuation of item 3 of first sheet)

This International Searching Authority found multiple inventions in this international application, as follows:
see extra sheet

1. ☐ As all required additional search fees were timely paid by the applicant, this international search report covers all searchable claims.

2. ☐ As all searchable claims could be searched without effort justifying additional fees, this Authority did not invite payment of additional fees.

3. ☐ As only some of the required additional search fees were timely paid by the applicant, this international search report covers only those claims for which fees were paid, specifically claims Nos.:

4. ☒ No required additional search fees were timely paid by the applicant. Consequently, this international search report is restricted to the invention first mentioned in the claims; it is covered by claims Nos.:
1-13

Remark on Protest

☐ The additional search fees were accompanied by the applicant's protest and, where applicable, the payment of a protest fee.

☐ The additional search fees were accompanied by the applicant's protest but the applicable protest fee was not paid within the time limit specified in the invitation.

☐ No protest accompanied the payment of additional search fees.

INTERNATIONAL SEARCH REPORT

International application No.
PCT/US 18/30491

Continuation of Box No III Observations where unity of invention is lacking

This application contains the following inventions or groups of inventions which are not so linked as to form a single general inventive concept under PCT Rule 13.1. In order for all inventions to be examined, the appropriate additional examination fees must be paid.

Group I: Claims 1-13 drawn to an apparatus for generating electricity from solar radiation.

Group II: Claims 14-15, drawn to a broadband antireflection coating for fused silica.

Group III: Claim 16, drawn to a method for broadband antireflection coating of a hot-pressed high-borate.

Group IV: Claims 17-18, drawn to a method for forming as a single piece, a glass lens array.

Group V: Claims 19-21, drawn to a method for forming a lens array from individual lenses.

Group VI: Claims 22, 24, drawn to a drawn to a dual axis, altitude-azimuth tracker to carry solar reflectors.

The inventions listed in the above-mentioned groups do not relate to a single general inventive concept under PCT Rule 13.1 because, under PCT Rule 13.2, they lack the same or corresponding special technical features for the following reasons:

Special Technical Features
Group I includes the special technical feature of photovoltaic cells are configured to convert said sunlight into electricity after being concentrated and divided between said photovoltaic cells in two imaging stages, not included in the other groups.

Group II includes the special technical feature of two successively deposited sol-gel layers of different refractive index, both indices being less than that of silica, not included in the other groups.

Group III includes the special technical feature of preparing a lens by phase separation, by heat-treating at 570-650 degrees C for 6-24 hours, then removing the molding contamination by soaking in 5-15% ammonium bifluoride, not included in the other groups.

Group IV includes the special technical feature of preparing a mold having a first face with a multiplicity of sharp boundaries to form a first, quilted surface of the contiguous lenses of a lens array, and a second smoothly curved face, not included in the other groups.

Group V includes the special technical feature of cutting individual lenses into individual, differently-shaped lens segments, not included in the other groups.

Group VI includes the special technical feature of a rigid triangular azimuth spaceframe structure with wheels, not included in the other groups.

Common Technical Features:
The only technical features shared by Groups I and VI that would otherwise unify the groups, are solar reflectors. However, these shared technical features do not represent a contribution over prior art, because the shared technical features are disclosed by US 2008/0185034 A1 (Corio).

The only additional technical feature shared by Groups I, IV and V that would otherwise unify the groups, is a fly's eye lens (lens array). However, this shared technical feature does not represent a contribution over prior art, because the shared technical feature is disclosed by Corio

Corio discloses solar reflectors and a fly's eye lens (para [0046]-[0047]: Primary lens sheet 48 is configured similarly to a fly's eye with a matrix of many small lenses...a rectangular reflective secondary lens 72 is disposed between primary lens 54 and active surface 22 of PV cells 20).

As the common technical features were known in the art at the time of the invention, these cannot be considered special technical features that would otherwise unify the groups.

Therefore, Groups I-VI lack unity under PCT Rule 13.

Note: Claim 23 is held unsearchable because it is a dependent claim and is not drafted in accordance with the second and third sentences of Rule 6.4(a).